Apoptosis (2019) 24:478–498
https://doi.org/10.1007/s10495-019-01530-2

Inhibition of TNF-α-induced neuronal apoptosis by antidepressants acting through the lysophosphatidic acid receptor LPA_1

Maria C. Olianas[1] · Simona Dedoni[1] · Pierluigi Onali[1,2]

Published online: 6 March 2019

Abstract

Tumor necrosis factor-α (TNF-α), a pro-inflammatory cytokine considered to be implicated in the pathogenesis of major depressive disorder, is a critical regulator of neuronal cell fate. In the present study we found that TNF-α-induced apoptosis of HT22 hippocampal cells, a neuroblast-like cell line, was markedly attenuated by the antidepressants mianserin, mirtazapine and amitriptyline. The anti-apoptotic effect of the antidepressants was blocked by either pharmacological inhibition or gene silencing of the lysophosphatidic acid receptor LPA_1. Mianserin failed to affect TNF-α-induced caspase 8 activation, but inhibited the loss of mitochondrial membrane potential, the release of cytochrome c from mitochondria, procaspase 9 cleavage and downstream activation of caspase 3 in response to the cytokine. By acting through LPA_1, mianserin also attenuated the enhanced pro-apoptotic response induced by the combination of TNF-α with other pro-inflammatory cytokines. TNF-α appeared to counterbalance its own pro-apoptotic response by activating NF-kB, ERK1/2 and JNK. Antidepressants had no significant effects on NF-kB activation, but potentiated the TAK-1-dependent phosphorylation of ERK1/2 and JNK elicited by the cytokine. This synergistic interaction was associated with enhanced JNK-mediated phosphorylation of Bcl-2 at Ser70 and increased ERK1/2-dependent mitochondrial accumulation of Mcl-1, two anti-apoptotic proteins that promote mitochondrial outer membrane stability. These results indicate that certain antidepressants, by activating LPA_1 signalling, protect HT22 hippocampal cells from TNF-α-induced apoptosis through a mechanism involving, at least in part, the potentiation of the pro-survival pathways activated by the cytokine.

Keywords TNF-α · Antidepressants · LPA_1 · HT22 hippocampal cells · Apoptosis

Introduction

Tumor necrosis factor (TNF)-α is a cytokine that acts as a major mediator of acute and chronic inflammation both in peripheral tissues and central nervous system (CNS) [1, 2]. As a component of the innate immune system, TNF-α is produced in response to infection, tissue injury or cellular dysfunction by different cell types, including astrocytes and microglia, and is expressed as soluble or membrane-bound form, which can be released following proteolytic cleavage by TNF-α cleaving enzyme. TNF-α exerts a variety of biological actions through the activation of two distinct transmembrane receptors, termed TNFR1 and TNFR2, which possess both different and overlapping signalling properties [1–3]. While TNFR1 is expressed in many cell types and can be activated by both soluble and membrane-bound forms of TNF-α, TNFR2 is present in a limited population of immune, endothelial and nerve cells and is preferentially activated by the membrane-bound form of the cytokine [4]. Moreover, as a member of the death receptor family, TNFR1 possesses a cytoplasmic death domain, which can bind the adaptor proteins TRADD and FADD and trigger either pro-apoptotic or anti-apoptotic responses. Conversely, the TNFR2 intracellular region is devoid of the death domain and predominantly recruits the E3 ubiquitin ligase TRAF-2 that signals through the NF-kB pro-survival pathway [1–3].

Electronic supplementary material The online version of this article (https://doi.org/10.1007/s10495-019-01530-2) contains supplementary material, which is available to authorized users.

✉ Pierluigi Onali
onali@unica.it

[1] Laboratory of Cellular and Molecular Pharmacology, Section of Neurosciences, Department of Biomedical Sciences, University of Cagliari, Cagliari, Italy

[2] Department of Biomedical Sciences, University of Cagliari, Cittadella Universitaria, 09042 Monserrato, CA, Italy

Besides its peripheral actions in innate immune responses and inflammatory processes, TNF-α can affect CNS function under both physiological and pathological conditions [5–7]. Depending on TNFR1 or TNFR2 activation, cell type and the actions of concomitant stimuli, exposure to TNF-α can either protect cultured neurons from different injuries [8–11] or exert direct and indirect neurotoxic effects [12–17]. A number of studies employing neurotoxicant and transgenic animal models of neurodegenerative diseases and clinical findings have provided substantial evidence that elevated brain levels of TNF-α and / or dysregulated TNF-α signalling exert neurotoxic effects and may play a role in the sustained inflammatory reactions contributing to Parkinson's disease, Alzheimer's disease, multiple sclerosis and amyotrophic lateral sclerosis [6, 14]. Compounds targeting TNFα/TNFR1 signalling may constitute novel therapeutic tools for peripheral and central inflammatory diseases [18].

An overactive TNF-α signalling and a pro-inflammatory state may also occur in major depressive disorder [19]. Thus, elevated serum levels of inflammatory mediators, along with enhanced acute-phase proteins and increased expression of chemokines and adhesion molecules, have been detected in depressed patients [20, 21]. Moreover, preclinical studies have shown that in mice gene deletion of either TNFR1 or TNFR2 leads to antidepressant-like behaviour [22] and that TNF-α increases anxiety-like responses in virally-infected animals [23]. Multiple mechanisms of action may mediate the pro-depressant effects of TNF-α and other pro-inflammatory cytokines [24], including direct impairment of hippocampal neural progenitor cell development and survival [25–27].

Because of the potential causative role of TNF-α in major depression, an important issue is to understand how its action can be affected by drugs commonly employed to treat this disorder. There is evidence that different classes of antidepressants inhibit the production of pro-inflammatory cytokines, including TNF-α, in cultured cell systems and in animal models of depression [28–30]. However, there is little information on whether antidepressants are capable of counteracting the deleterious effect of TNF-α/TNFR signalling on neuronal cell survival.

We have recently reported that in different cellular systems distinct classes of antidepressants induce growth factor receptor trans-activation and stimulate cell proliferation and survival through a novel mechanism involving the activation of the lysophosphatidic acid receptor LPA_1 [31–33]. This receptor is present in different cell types within the developing and mature central nervous system [34], and in animal models deletion of LPA_1 has been associated with behavioural alterations, including anxiety and depression [35].

In the present study we provide evidence that in mouse HT22 hippocampal cells, a neuroblast-like cell line, the antidepressants mianserin, mirtazapine and amitriptyline counteract the pro-apoptotic action of TNF-α/TNFR1 by acting through LPA_1.

Materials and methods

Materials

Recombinant mouse TNF-α, human TNF-α and mouse interferon (IFN)-β were purchased from ProSpec-Tany TechnoGene Ltd (Ness Ziona, Israel). Recombinant mouse IFN-γ, interleukin (IL)-1a and IL-6 were from Immuno-Tools (Friesoythe, Germany). Mianserin hydrochloride, mirtazapine hydrochloride, amitriptyline hydrochloride and 4′,6-diamidino-2phenylindole dihydrochloride (DAPI) were obtained from Sigma–Aldrich (St. Louis, MO, USA). Ki16425, PD173074 and 5Z-7-oxozeaenol were from Santa Cruz Biotechnology (Dallas, TX, USA). AM966 was purchased from ChemScene (Monmouth Junction, NJ, USA). 1-Oleoyl-lysophosphatidic acid (LPA) was from Santa Cruz Biotechnology and Sigma–Aldrich. Ro-6842262, TCS JNK 6o and PD98059 were obtained from Tocris Bioscience (Bristol, UK). BIRB0796 was from Axon Medchem BV (Groningen, The Netherlands). BAY 11-7085 was from SelleckChem (Houston, TX, USA).

Cell culture

HT22 hippocampal cells were a generous gift of Dr. David Schubert (The Salk Institute, La Jolla, CA, USA). The cells were grown in DMEM medium supplemented with 10% foetal calf serum (FCS) and 0.5% penicillin/streptomycin (Sigma–Aldrich) at 37 °C in a humidified atmosphere of 5% CO_2 in air.

Cell transfection

HT22 cells were transfected with either mouse LPA_1 siRNA or control siRNA-A (Santa Cruz Biotechnology). Cells were incubated with siRNA duplexes (75 nM) for 12 h by using Lipofectamine RNAiMAX (Invitrogen/Life Technologies) as transfection reagent. Transfection efficiency was determined in parallel samples treated with fluorescein-conjugated control siRNA-A (Santa Cruz Biotechnology). An efficiency of ~65% was obtained in five separate experiments. Cell transfections with pCMV-myc-ERK2-L4A-MEK1 fusion construct (ERK2-CA) (Addgene, Cambridge, MA, USA), a constitutively active form of ERK2 [36], were performed as previously described [37]. Cells were used 48 h post-transfection.

Isolation of cell nuclei and mitochondria

For isolation of cell nuclei, HT22 cells grown in 100 mm petri dishes were treated with the agents as indicated, washed with ice-cold phosphate-buffered saline (PBS) (pH 7.4) and scraped in a ice-cold lysis buffer containing 10 mM Tris–HCl, 2 mM $MgCl_2$, 10 mM NaCl, 0.5 mM EGTA, 2 mM sodium orthovanadate, 10 mM sodium fluoride, 1 mM phenylmethylsulfonyl fluoride (PMSF), 0.05% Nonidet P-40, 0.1% phosphatase inhibitor cocktail 3 and 1% protease inhibitor cocktail (Sigma–Aldrich) (pH 7.4). Cell lysates were centrifuged at 3000×*g* for 10 min at 4 °C, the supernatant was collected and centrifuged at 24,000×*g* for 20 min to obtain a cytosolic fraction. The pellets were washed three times in ice-cold washing buffer containing 10 mM Pipes/NaOH, 300 mM sucrose, 2 mM $MgCl_2$, 10 mM NaCl, 0.5 mM EGTA, 2 mM sodium orthovanadate, 10 mM sodium fluoride, 1 mM PMSF, 0.1% phosphatase inhibitor cocktail 3 and 1% protease inhibitor cocktail (pH 7.4) and layered over a cushion of 1 ml of sucrose buffer containing 1 M sucrose, 2 mM sodium orthovanadate, 10 mM sodium fluoride, 1 mM PMSF, 0.1% phosphatase inhibitor cocktail 3 and 1% protease inhibitor cocktail. Following centrifugation at 3000×*g* for 10 min at 4 °C, the nuclei present in the pellets were washed and the nuclear proteins were extracted by incubating the nuclei on ice for 30 min in a buffer containing 20 mM Hepes/NaOH, 300 mM NaCl, 2 mM $MgCl_2$, 0.2 mM EDTA, 2 mM sodium orthovanadate, 10 mM sodium fluoride, 1 mM PMSF, 0.1% phosphatase inhibitor cocktail 3 and 1% protease inhibitor cocktail (pH 7.9). Following centrifugation at 24,000 × *g* for 10 min at 4 °C, the supernatant containing the nuclear extract was mixed with sample buffer and analyzed by Western blot.

A crude mitochondrial fraction was prepared as previously described [38] with some modifications. Briefly, HT22 cells grown to 80% confluency were treated as indicated, detached by incubation in PBS-EDTA, collected by centrifugation at 50 x g for 5 min and resuspended in a homogenization buffer containing 220 mM mannitol, 250 mM sucrose, 50 mM Pipes/KOH (pH 7.4), 50 mM KCl, 5 mM EGTA, 2 mM $MgCl_2$, 1 mM dithiothreitol, 1 mM PMSF and 1% protease inhibitor cocktail. Following 30 min incubation at ice-bath temperature, cells were lysed by using a glass/glass Dounce tissue grinder and pestle B (100 strokes) and centrifuged 1000×*g* for 10 min 4 °C. The supernatant was collected and centrifuged at 14,000×*g* for 15 min at 4 °C. The pellet containing the mitochondrial fraction was resuspended by sonication in RIPA buffer, whereas the supernatant was taken as the cytosolic fraction. Both fractions were diluted 1:5 in 5× sample buffer and analyzed by Western blotting.

Western blot analysis

HT22 cells were treated as specified in the text and cell lysates were prepared by scraping the cells in an ice-cold RIPA buffer containing phosphate-buffered saline (PBS), 0.1% sodium dodecyl sulphate (SDS), 1% Nonidet P-40, 0.5% sodium deoxycholate, 2 mM EDTA, 2 mM EGTA, 4 mM sodium pyrophosphate, 2 mM sodium orthovanadate, 10 mM sodium fluoride, 20 nM okadaic acid, 0.5% phosphatase inhibitor cocktail 3, 1% protease inhibitor cocktail and 1 mM PMSF. Following sonication for 5 s, protein concentration was determined by the Bio-Rad protein assay (Bio-Rad Lab., Hercules, CA, USA). Cell proteins were separated by SDS–polyacrylamide gel electrophoresis and electrophoretically transferred to either polyvinylidene difluoride or nitrocellulose membranes. Membranes were incubated overnight at 4 °C with one of the following primary antibodies: extracellular signal-regulated kinase1 and 2 (ERK1/2), phospho-Jun-N-terminal kinase (JNK) (Thr183/Tyr185), phospho-p38 MAPK (Thr180/Tyr182), cleaved caspase 9 (Asp330), procaspase 9, cleaved caspase 3 (Asp175), procaspase 3, cleaved poly-(ADP ribose) polymerase (PARP) (Asp214), PARP, phospho-IkB-α (Ser32), IkB-α, phospho-NF-kB p65 (Ser536), NF-kB p65, phospho-Mcl-1(Thr163), phospho-Bcl-2 (Ser70) (Cell Signaling Technology, Beverly, MA, USA); TNFR1 (sc-8436), LPA_1 (sc-515665), cytochrome c oxidase IV (CYT IV) (sc-69359), JNK (sc-571), Bcl-2 (sc-7382), transforming growth factor-β-activated kinase-1 (TAK1) (sc-7967), Mcl-1 (sc-819), STAT1 p84/p91 (sc-592), phospho-STAT3 (Tyr705) (sc-8059) (Santa Cruz Biotechnology); phospho-ERK1 (Thr202/Tyr204) / ERK2 (Thr185/Tyr187) (Neuromics, Northfield, MN, USA); phospho-STAT1 (Tyr701), phospho-TAK1 (Thr184/187) (Thermo Scientific, Rockford, IL, USA); cytochrome c (Millipore, Temecula, CA, USA); STAT3 (Zymed Laboratories, San Francisco, CA, USA); actin (Sigma–Aldrich); glyceraldehyde 3-phosphate dehydrogenase (GAPDH) (Synaptic Systems, Gottingen, Germany). Following incubation with horseradish peroxidase-conjugated secondary antibodies (Santa Cruz Biotechnology), immunoreactive bands were detected by using Clarity Western ECL substrate (Bio-Rad Lab.) and ECL Hyperfilm (Amersham). Band densities were determined by densitometric analysis using Image Scanner III (GE Healthcare, Milan, Italy) and NIH ImageJ software (US National Institutes of Health, Bethesda, MD, USA). The optical density of phosphoproteins was normalized to the density of the corresponding total protein in the same samples. For analysis of cleaved caspases and PARP the formation of the cleaved protein was normalized to the level of the procaspase or uncleaved PARP determined in the same samples. For the remaining proteins, the densitometric values were normalized to the levels of either actin or GAPDH.

Immunofluorescence analysis

For analysis of cleaved caspase 3 expression HT22 cells plated on poly-L-lysine-pre-coated glass coverslips were incubated with the test compounds at 37 °C as specified in the text. Cells were washed, fixed with 4% paraformaldehyde and permeabilized with 0.2% Triton X-100. Cells were then blocked with 3% BSA and 1% normal goat serum and incubated overnight at 4 °C with rabbit anti-cleaved caspase 3 (1:200) (Cell Signaling Technology). For analysis of receptor expression, HT22 cells were fixed as described above and then dually labelled with goat anti-LPA_1 (sc-22207) (1:100) and mouse anti-TNFR1(sc-8436) (1:200) antibodies (Santa Cruz Biotechnology), both directed against an extracellular epitope of the receptor. To study NF-kB p65 translocation, cells were treated with the test agents, fixed, permeabilized, and incubated with rabbit anti-NF-kB p65 antibody (1:200) (Cell Signaling Technology) and mouse anti-neurofilament 160/200 (NF160/200) antibody (1:500) (Sigma –Aldrich).

Cells were then incubated with the appropriate Alexa-Fluor488- or Alexa-Fluor594-conjugated secondary antibodies (Invitrogen-Molecular Probes) and cell nuclei were stained with 0.1 µg/ml DAPI. Cells were analyzed with an Olympus BX61 microscope equipped with a F-View II CCD-camera by using either a × 40 or a × 60 objective lens. Digital images were acquired using constant camera settings within each experiment and were analyzed using the program Cell P (Olympus Soft Imaging Solutions, Homburg, Germany). For quantification, at least ten fields were randomly selected for each sample and only cells showing an unobstructed nucleus or soma were considered. In these cells, the average pixel intensity was measured within the region of the nucleus or the cell soma and in an adjacent area, which was used as background value. Cells were deemed to be positive if the average pixel intensity was equal or above a threshold value corresponding to one standard deviation above the average pixel intensity of the corresponding control samples [39]. No labelling was detected in samples treated without primary antibodies. Five separate HT22 cell cultures were analyzed by an investigator unaware of the treatment.

Analysis of living cell morphology

HT22 cells were grown in 6-well plates and treated as specified in the text. The morphology of living cells was analyzed by phase-contrast light microscopy using an Olympus IX 51 inverted microscope equipped with Plan achromatic objectives. Images were acquired in randomly selected fields by using an Olympus digital camera. Images were analyzed by an investigator unaware of the treatment.

Assay of caspase activity

HT22 cells grown in 96-well plates (ViewPlate-96, PerkinElmer, Waltham, MA, USA), were incubated as specified in the text. Cells were then assayed for caspase activity by using Caspase-Glo 8 and 3/7 assay kits (Promega, Madison, WI, USA), following the manufacturer's instructions. Luminescence intensity was measured by using a Wallac Victor III microplate reader (PerkinElmer). Assays were performed in triplicate.

Assay of cell viability

Cell viability was determined by either cytofluorimetric analysis using the Muse Cell Count and Viability kit (Millipore) or luminescence analysis using the Real Time-GLO MT assay kit (Promega, Madison, WI, USA). For cytofluorimetric assays, HT22 cells were treated with the experimental agents as specified in the text, detached by trypsin/EDTA treatment, washed with 10% FCS-containing medium and processed as specified by the manufacturer's protocols. Cells were analyzed by using the Muse Cell Analyzer (Millipore). Assays were performed in triplicate. For luminescence analysis, HT22 cells grown in 96-well plates (ViewPlate, PerkinElmer) were incubated with the reagents provided by the Real Time-Glo MT assay kit (Promega) in the presence of the test agents for 24 h. Luminescence intensity was measured as specified above. Assays were performed in triplicate.

Analysis of annexin V labelling

HT22 cells were treated for 16 h with the test agents, detached by trypsinization, collected by centrifugation and resuspended in growing medium containing 5% FCS. Cells were incubated with the Annexin & Dead Cell Kit reagent (Millipore). Data were acquired by counting 2000 events and analyzed by using the Muse Cell Analyzer as specified by the manufacture's instructions.

Analysis of mitochondrial membrane potential

HT22 cells were grown in 12-well plates, treated for 24 h with the test agents, collected by trypsinization, washed and incubated with the Muse Mitopotential Dye (Millipore) for 20 min at 37 °C. Thereafter, the cells were incubated with the dead cell marker 7-AAD (Millipore) for 5 min. Data were acquired by counting 5000 events and analyzed with the Muse Cell Analyzer.

Terminal transferase dUTP nick end-labeling assay (TUNEL assay)

HT22 cells grown on glass coverslips were incubated with the test agents for 24 h. In situ TUNEL assay was performed using the DeadEnd fluorimetric TUNEL system (Promega), according to the manufacturer's instructions. Cell nuclei were stained with DAPI. Images were captured over randomly selected fields and analyzed with Cell P software as described for cleaved caspase 3. Three separate culture preparations were analyzed.

Statistical analysis

Results are reported as the mean ± SEM of n independent experiments. Concentration–response curves were analyzed by the program Graph Pad Prism (San Diego, CA, USA), which yielded the drug concentration producing half-maximal stimulation (EC_{50}) or half-maximal inhibition (IC_{50}). Unless otherwise indicated, data are expressed as percentage or fold stimulation of control, which was included in each independent experiment. The control group was set as 100 or 1 with a variance obtained by expressing each control value as a percentage of the mean of the raw values of the control group. In the experiments where control values were equal to zero, values of experimental groups were expressed as a percentage of the maximal effect set as 100. The variance of this value was determined in the same manner as for the control group. Statistical analysis was performed by using one way analysis of variance (ANOVA) followed by Newman–Keuls post hoc test. A value of $p < 0.05$ was considered as the level of statistical significance.

Results

HT22 hippocampal cells co-express TNFR1 and LPA_1

Immunofluorescence analysis of HT22 hippocampal cells showed that TNFR1 immunoreactivity was expressed in a large population (65%) of cells examined and was characterized as a dotted staining distributed diffusely on the cell soma (Fig. 1a). A major fraction of total cells (70%) displayed LPA_1 immunoreactivity, which appeared mainly concentrated in restricted areas of the cell body and surface membrane and consistently co-localized with TNFR1 labelling (Fig. 1a).

Antidepressants inhibit TNF-α-induced apoptosis of HT22 cells through LPA_1

Phase-contrast light microscopy showed that prolonged exposure (24 h) to TNF-α (10 ng/ml) induced cell rounding, shrinking and detachment from the substrate, indicating loss of cell viability (Fig. 1b). These morphological alterations were prevented in the presence of the tetracyclic antidepressant mianserin (5 μM), which per se had no effect. Addition of the selective LPA_1 antagonist AM966 (100 nM) failed to alter cell morphology but completely blocked the protective effect of the antidepressant. Quantitative analysis by flow cytometry indicated that TNF-α decreased cell viability by about 50% ($p < 0.001$) (Fig. 1c–e). A comparable cytotoxic effect was observed following cell treatment with human TNF-α, which selectively activates murine TNFR1 over TNFR2 [40] (Online Resource 1). Mianserin (5 μM) and mirtazapine (20 μM), a structurally similar antidepressant, counteracted the cell death induced by TNF-α, and blockade of LPA_1 with AM966 prevented the pro-survival activity of these drugs (Fig. 1c, d). Similar results were obtained when the effects on cell viability were determined by using a luminescence assay performed on cell monolayers (Online Resource 2). Western blotting experiments indicated that the prolonged exposure of HT22 hippocampal cells to either mianserin (5 μM) or mirtazapine (20 μM) in the absence and in the presence of TNF-α failed to affect the expression levels of TNFR1 (Online Resource 3).

We have previously shown that in HT22 hippocampal cells both mianserin and mirtazapine activate the MAP kinase ERK1/2 through LPA_1 [33]. The tricyclic antidepressant amitriptyline was similarly effective in stimulating ERK1/2 phosphorylation displaying an EC_{50} value of 3.2 ± 0.4 μM (n = 4) (Online Resource 4). The stimulatory effect of amitriptyline (10 μM) was completely antagonized by the $LPA_{1/3}$ receptor blocker Ki16425 ($IC_{50} = 62 \pm 5$ nM, n = 5) and greatly reduced by AM966 ($76 \pm 5\%$ inhibition at 1 μM, $IC_{50} = 6.1 \pm 0.4$ nM, n = 4) (Online Resource 4). Moreover, another selective LPA_1 antagonist, Ro6842262 [41], tested at the concentration of 100 nM, suppressed ERK1/2 activation elicited by either mianserin (5 μM) or amitriptyline (10 μM) (Online Resource 4). As observed with mianserin and mirtazapine, cell treatment with amitriptyline counteracted TNF-α-induced HT22 hippocampal cell death and this protective effect was antagonized by AM966 (Fig. 1e).

The binding of annexin V to phosphatidylserine expressed at the external cell surface is a marker of apoptotic death. As shown in Fig. 1f, prolonged exposure of HT22 hippocampal cells to TNF-α (10 ng/ml) caused a marked increase in the percentage of cells positively stained with annexin V, which was prevented by

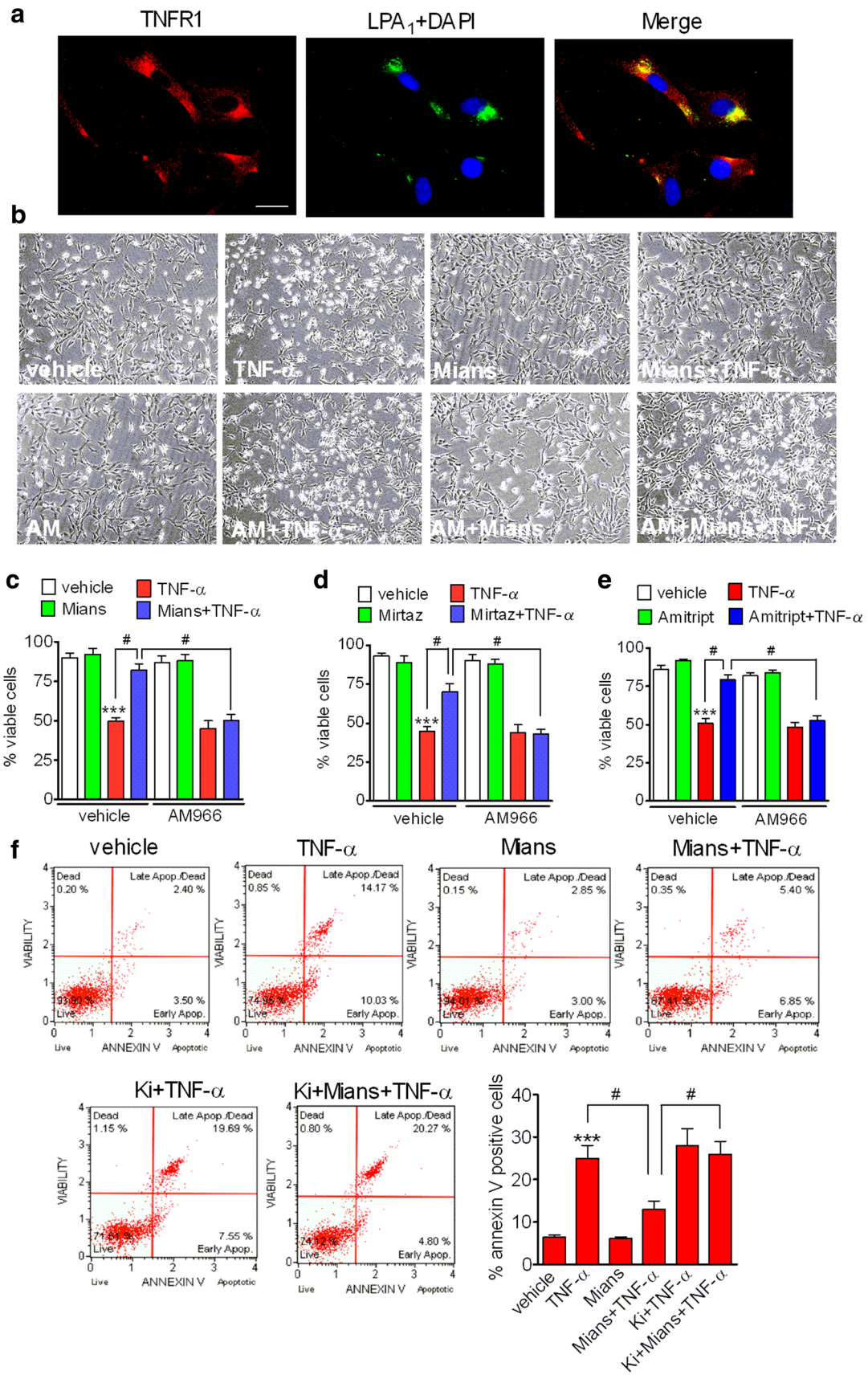
a
TNFR1
LPA1+DAPI
Merge
b
vehicle
TNF-α
Mians
Mians+TNF-α
AM
AM+TNF-α
AM+Mians
AM+Mians+TNF-α
c
vehicle
TNF-α
Mians
Mians+TNF-α
% viable cells
vehicle
AM966
d
vehicle
TNF-α
Mirtaz
Mirtaz+TNF-α
% viable cells
vehicle
AM966
e
vehicle
TNF-α
Amitript
Amitript+TNF-α
% viable cells
vehicle
AM966
f
vehicle
TNF-α
Mians
Mians+TNF-α
Ki+TNF-α
Ki+Mians+TNF-α
VIABILITY
ANNEXIN V
Dead
Late Apop./Dead
Live
Early Apop.
Apoptotic
% annexin V positive cells
vehicle
TNF-α
Mians
Mians+TNF-α
Ki+TNF-α
Ki+Mians+TNF-α

◂**Fig. 1** Antidepressants inhibit TNF-α-induced neuronal death via LPA_1. **a** Immunofluorescence analysis of TNFR1 and LPA_1 expression in HT22 hippocampal cells. Images are representative of three separate experiments. The yellow color indicates TNFR1 and LPA_1 co-localization. Bar = 25 μm. **b** HT22 hippocampal cells incubated in medium containing 10% FCS were pre-treated with either vehicle or 100 nM AM966 (AM) for 30 min and then with either vehicle or 5 μM mianserin (Mians) for 1 h. Thereafter, cells were exposed to either vehicle or 10 ng / ml TNF-α for 24 h. Cells were analyzed by phase-contrast microscopy. Images are representative of four similar experiments. Magnification: ×40. **c**–**e** HT22 cells were pre-incubated for 30 min with either vehicle or 100 nM AM966 and then treated for 1 h with either vehicle, 5 μM mianserin, 20 μM mirtazapine (Mirtaz), or 10 μM amitriptyline (Amitript). Thereafter, the cells were exposed for 24 h to 10 ng/ ml TNF-α. Cells were analyzed for viability by a cytofluorimetric assay. Values are the mean ± SEM of four experiments. **f** cells were pre-incubated for 30 min with either vehicle or 100 nM Ki16425 and then treated with vehicle or 5 μM mianserin for 1 h. Thereafter the cells were exposed for 16 h to either vehicle or 10 ng/ml TNF-α. Values are reported as percent of annexin V positive cells (early apoptotic + late apoptotic cells) and are the mean ± SEM of four experiments. ***$p < 0.001$ versus control (vehicle), $^{\#}p < 0.05$

pre-treatment with mianserin (5 μM). The addition of Ki16425 (100 nM) abolished the anti-apoptotic effect of the antidepressant.

Mianserin fails to inhibit TNF-α-induced activation of caspase 8

A well known mechanism by which TNF-α can cause apoptotic cell death is the sequential recruitment of the cytoplasmic adapter proteins TRADD and FADD to the dead domain of TNFR1, which then promote the activation of caspase 8 and the initiation of the apoptotic cascade [1, 2]. Exposure of HT22 hippocampal cells to TNF-α (10 ng/ml) induced a significant increase of caspase 8 activity (Fig. 2a), which is consistent with previous studies [15]. This response was not affected by pre-treatment with mianserin, indicating that the anti-apoptotic effect elicited by the antidepressant was exerted at a level located downstream of caspase 8 activation.

Mianserin blocks TNF-α-induced cytochrome c release

Activation of caspase 8 can cleave the pro-apoptotic protein Bid generating a truncated carboxy-terminal fragment, which triggers the intrinsic apoptotic cascade by inducing the release from mitochondria of pro-apoptotic factors including cytochrome c [42]. As shown in Fig. 2b, c, cell fractionation experiments indicated that in HT22 hippocampal cells TNF-α induced cytochrome c release from mitochondria and this effect was inhibited by cell pre-treatment with mianserin in a manner that was sensitive to blockade by AM966.

Loss of mitochondrial membrane potential is an index of increased mitochondrial outer membrane permeabilization and a key event in the intrinsic apoptotic pathway [43]. As shown in Fig. 2d, TNF-α increased the percentage of HT22 hippocampal cells with a decreased mitochondrial membrane potential. Mianserin significantly reduced the response to TNF-α in the absence but not in the presence of Ki16425 (100 nM).

Antidepressants inhibit TNF-α-induced activation of caspases 9 and 3 through LPA_1

The release of cytochrome c triggers the formation of the apoptosome and the consequent activation of caspase 9, which then processes and activates the effector caspases 3 and 7 [43]. Treatment of HT22 hippocampal cells with TNF-α promoted a strong activation of caspase 9, as indicated by the increased formation of the cleaved active fragment of 37 kDa (Fig. 3a). Pre-treatment with either mirtazapine, mianserin or amitriptyline inhibited TNF-α-induced caspase 9 activation and this effect was antagonized by AM966. TNF-α stimulated the activation of caspase 3, as indicated by the accumulation of the active fragments of 19 and 17 kDa (Fig. 3b), and by direct measurement of caspase 3/7 activity (Fig. 3c). In both assays, mianserin (5 μM) markedly reduced TNF-α-induced caspase activation, an effect that was prevented by LPA_1 blockade with either AM966 (100 nM) (Fig. 3b) or Ro6842262 (100 nM) (Fig. 3c). These results were further corroborated by immunofluorescence analysis which showed that TNF-α increased the percentage of HT22 hippocampal cells positive for cleaved caspase 3 and that mianserin exerted a protective effect in cells pre-treated with vehicle but not with AM966 (Fig. 3d).

LPA_1 mediates antidepressant-induced inhibition of TNF-α-stimulated PARP cleavage and DNA fragmentation

Proteolytic cleavage of the DNA-repairing enzyme PARP by activated effector caspases and DNA fragmentation are hallmarks of apoptotic cell death. TNF-α greatly stimulated the accumulation of the 89 kDa fragment of PARP, which is the product of cleavage at Asp214 (Fig. 3e, f). Mianserin and amitriptyline counteracted the stimulation of PARP cleavage by TNF-α and their effect was prevented by AM966 and Ro6842262, respectively (Fig. 3e, f). To further examine the involvement of LPA_1 in the antidepressant anti-apoptotic effect, HT22 hippocampal cells were treated with siRNA duplexes to knockdown LPA_1. This treatment reduced the expression levels of LPA_1 by approximately 75%, and attenuated the inhibitory effect of mianserin on TNF-α-induced PARP cleavage, as compared to control siRNA-treated cells (Fig. 3g, h).

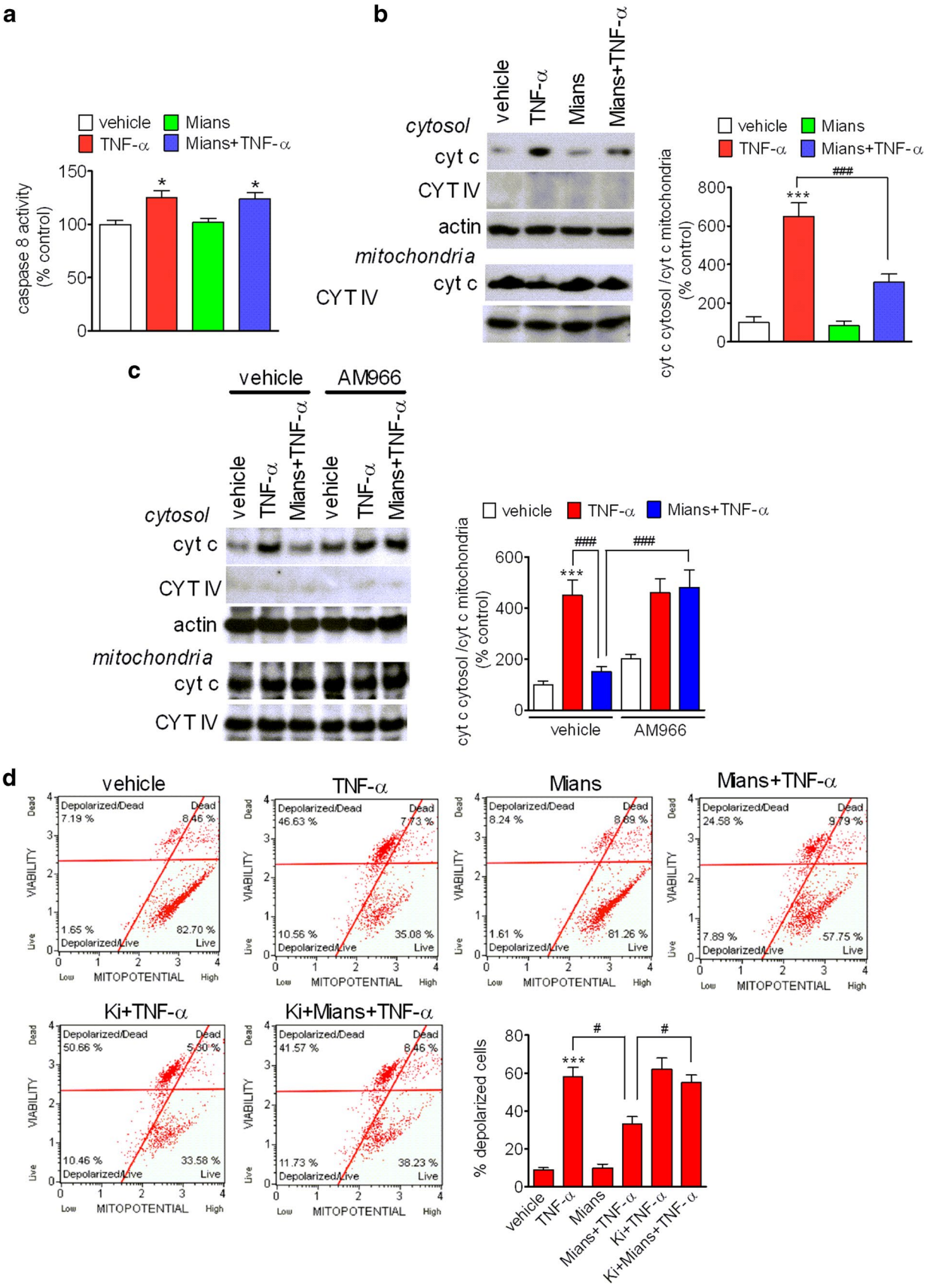
a
vehicle
Mians
TNF-α
Mians+TNF-α
caspase 8 activity (% control)
150
100
50
0
*
*
b
vehicle
TNF-α
Mians
Mians+TNF-α
cytosol
cyt c
CYT IV
actin
mitochondria
cyt c
CYT IV
vehicle
Mians
TNF-α
Mians+TNF-α
cyt c cytosol /cyt c mitochondria (% control)
800
600
400
200
0
***
###
c
vehicle
AM966
vehicle
TNF-α
Mians+TNF-α
vehicle
TNF-α
Mians+TNF-α
cytosol
cyt c
CYT IV
actin
mitochondria
cyt c
CYT IV
vehicle
TNF-α
Mians+TNF-α
cyt c cytosol /cyt c mitochondria (% control)
600
400
200
0
***
###
###
vehicle
AM966
d
vehicle
TNF-α
Mians
Mians+TNF-α
Depolarized/Dead
Dead
7.19 %
8.46 %
1.65 %
82.70 %
Depolarized/Live
Live
46.63 %
7.73 %
10.56 %
35.08 %
8.24 %
8.89 %
1.61 %
81.26 %
24.58 %
9.79 %
7.89 %
57.75 %
VIABILITY
Dead
Live
MITOPOTENTIAL
Low
High
Ki+TNF-α
Ki+Mians+TNF-α
50.66 %
5.30 %
10.46 %
33.58 %
41.57 %
8.46 %
11.73 %
38.23 %
% depolarized cells
80
60
40
20
0
***
#
#
vehicle
TNF-α
Mians
Mians+TNF-α
Ki+TNF-α
Ki+Mians+TNF-α

◂**Fig. 2** Mianserin fails to affect caspase 8 activation but inhibits cytochrome c release induced by TNF-α. **a** HT22 hippocampal cells were pre-treated for 1 h with either vehicle or 5 μM mianserin (Mians) and then exposed for 3 h to either vehicle or 10 ng / ml TNF-α. Caspase 8 activity was assayed by using a luminescence assay. Values are reported as percent of control (vehicle) and are the mean ± SEM of four experiments. **b** HT22 cells were pre-treated as indicated in a and then exposed for 16 h to either vehicle or 10 ng / ml TNF-α. Cytosolic and mitochondrial cell fractions were analyzed for cytochrome c (cyt c), cytochrome oxidase IV (CYT IV), and actin by Western blot. The levels of cytochrome c in the cytosolic fraction were normalized to the corresponding levels in the mitochondrial fractions and expressed as percent of control (vehicle). Values are the mean ± SEM of four independent experiments. **c** Cells were pre-incubated for 30 min with either vehicle or 100 nM AM966 and then treated for 1 h with either vehicle or 5 μM mianserin. Thereafter, cells were exposed for 16 h to 10 ng/ml TNF-α. Cytosolic and mitochondrial cell fractions were isolated and the release of cytochrome c in the cytosol was determined as described in b. Values are the mean ± SEM of three independent experiments. **d** Cells were treated as indicated in Fig. 1f. Mitochondrial membrane potential was determined by a cytofluorimetric assay. Values are reported as percent of depolarized cells (live + dead) and are the mean ± SEM of three independent experiments. $^{*}p < 0.05$, $^{***}p < 0.001$ versus control (vehicle), $^{\#}p < 0.05$, $^{\#\#\#}p < 0.001$

DNA fragmentation was significantly enhanced in HT22 hippocampal cells treated with TNF-α, as indicated by the increased percentage of cells which displayed a positive staining by in situ TUNEL assay (Fig. 3i). Mianserin completely inhibited this pro-apoptotic response in cells pre-treated with vehicle but not with AM966.

LPA_1 activation by mianserin counteracts the synergistic induction of apoptosis by the combination of pro-inflammatory cytokines

We next investigated the response of HT22 hippocampal cells to other pro-inflammatory cytokines, such as IFN-β, IFN-γ, IL-1a and IL-6. Cell exposure to these cytokines generated the expected intracellular signalling responses, as IFNs (30 ng/ml) and IL-6 (30 ng/ml) stimulated STAT1 and STAT3 Tyr-phosphorylation, respectively, whereas IL-1a (30 ng/ml) induced a rapid increase of p38 MAPK phosphorylation (Online Resource 5), indicating the presence of the cognate receptors. When added alone, IFN-β, IFN-γ, IL-6 and IL-1a failed to affect either caspase 9 or PARP cleavage, but significantly enhanced the stimulatory effect of TNF-α (Fig. 4a–c). Pre-treatment with mianserin (5 μM) attenuated the synergistic enhancement of PARP cleavage elicited by the combination of TNF-α with each of the other cytokines and the inhibitory effect of the antidepressant was blocked by either AM966 or Ki16425 (Fig. 4d–f).

Mianserin fails to affect TNF-α-induced activation of NF-kB

TNF-α is a major activator of the NF-kB transcription factors, which regulate a wide variety of pro-inflammatory genes and also induce the expression of different pro-survival proteins, thus counterbalancing the pro-apoptotic activity of the cytokine [1, 2, 44]. Activation of resting NF-kB factors complexed with the inhibitory IkB proteins in the cytoplasm is triggered by the phosphorylation and consequent proteasome-dependent degradation of IkB, which allows the release and nuclear translocation of active NF-kB dimers. As shown in Fig. 5a, in HT22 hippocampal cells TNF-α (10 ng / ml) induced a rapid phosphorylation of IkB-α at Ser32, which was associated with a marked decrease of IkB-α cellular content. Cell pre-treatment with mianserin (5 μM) had no effect per se on the levels of IkB-α and failed to affect the phosphorylation and degradation of the inhibitory protein induced by the cytokine. Immunofluorescence analysis showed that TNF-α induced a rapid translocation of the NF-kB p65 subunit from the cell cytosol to the nucleus, a response that remained largely unchanged by pre-treatment with mianserin (Fig. 5b). Cell fractionation experiments confirmed the lack of effect of mianserin on TNFα-induced nuclear translocation of NF-kB p65 subunit (Fig. 5c). TNF-α also caused a marked increase in the phosphorylation of NF-kB p65 at Ser536 located in the C-terminal transactivation domain, which has been shown to promote NF-kB p65 nuclear translocation and enhance its transcriptional activity [45]. Pre-treatment with mianserin had no effect on either basal or TNFα-stimulated p65 phosphorylation (Fig. 5c).

To investigate whether in HT22 hippocampal cells the activation of NF-kB by TNF-α affected the apoptotic response, cells were treated with Bay 11-7085, which prevents NF-kB activation by inhibiting IkB-α phosphorylation [46]. As shown in Fig. 5d, Bay 11-7085, tested at 1 and 10 μM, antagonized the down-regulation of IkB-α by TNF-α in a concentration-dependent manner. Cell treatment with 1 μM Bay 11-7085 significantly enhanced TNF-α-induced PARP cleavage, but did not prevent the inhibitory effect of mianserin on this response (Fig. 5e).

Inhibition of TNF-α-induced apoptosis by antidepressants involves FGF-R and ERK1/2 activities

In HT22 hippocampal cells activation of LPA_1 by antidepressants has been shown to induce the transactivation of FGF-R, which mediates the downstream activation of ERK1/2 pro-survival signalling [33]. As shown in Fig. 6a, blockade of FGF-R tyrosine kinase activity with the selective inhibitor PD173074 (30 nM) almost completely suppressed the

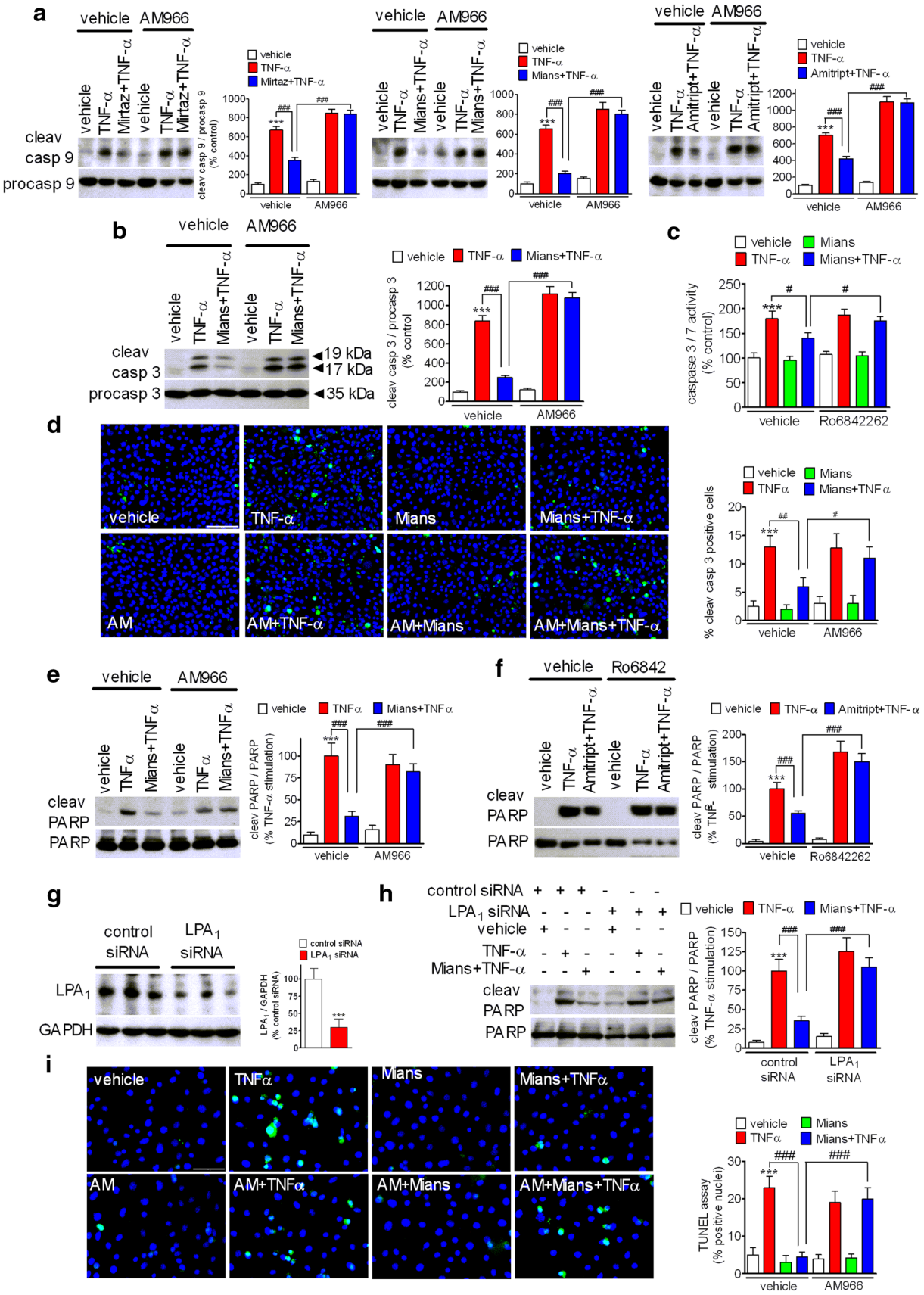
a
vehicle
AM966
vehicle
TNF-α
Mirtaz+TNF-α
Mians+TNF-α
Amitript+TNF-α
cleav
casp 9
procasp 9
cleav casp 9 / procasp 9 (% control)
b
cleav
casp 3
procasp 3
19 kDa
17 kDa
35 kDa
cleav casp 3 / procasp 3 (% control)
c
Mians
caspase 3 / 7 activity (% control)
Ro6842262
d
vehicle
TNF-α
Mians
Mians+TNF-α
AM
AM+TNF-α
AM+Mians
AM+Mians+TNF-α
% cleav casp 3 positive cells
e
TNFα
cleav PARP / PARP (% TNF-α stimulation)
f
Ro6842
g
control siRNA
LPA1 siRNA
GAPDH
LPA1 / GAPDH (% control siRNA)
h
control siRNA
LPA1 siRNA
i
TUNEL assay (% positive nuclei)

◂**Fig. 3** Antidepressants acting through LPA_1 inhibit the activation of caspases 9 and 3, PARP cleavage and DNA fragmentation induced by TNF-α. **a** HT22 hippocampal cells were pre-incubated with either vehicle or 100 nM AM966 for 30 min, treated for 1 h with either vehicle, 20 µM mirtazapine (Mirtaz), 5 µM mianserin (Mians) or 10 µM amitriptyline (Amitript) and then exposed for 24 h to either vehicle or 10 ng/ml TNF-α. The levels of cleaved caspase (cleav casp) 9 were normalized to the corresponding levels of procaspase (procasp) 9. Values are the mean ± SEM of four independent experiments. **b** cells were treated with AM966, mianserin and TNF-α as indicated in a. The total levels of the active cleaved caspase 3 fragments were normalized to the levels of procaspase 3. Values are the mean ± SEM of four independent experiments. **c** cells were pre-incubated for 30 min with either vehicle or 100 nM Ro1642262 and treated for 1 h with either vehicle or 5 µM mianserin. Cells were then exposed for 24 h to 10 ng /ml TNF-α. The activity of caspase 3/7 was determined by a luminescence assay. Values are the mean ± SEM of four experiments. **d** cells were sequentially treated with AM966, mianserin and TNF-α as indicated in a. Cleaved caspase 3 expression was analyzed by immunofluorescence (green color) and the percent of positive cells determined for each experimental condition. Values are the mean ± SEM of three independent experiments. **e** cells were treated with the indicated agents as specified in a. The levels of cleaved PARP were normalized to the corresponding levels of uncleaved PARP. Values are the mean ± SEM of four experiments. **f** cells were pre-incubated for 30 min with either vehicle or 100 nM Ro1642262 and then treated for 1 h with 10 µM amitriptyline. Thereafter, cells were exposed for 24 h to 10 ng/ml TNF-α. Values are the mean ± SEM of four experiments. **g** cells were transfected with either control siRNA or LPA_1 siRNA and the levels of LPA_1 were determined by Western blot 48 h post transfection. Each lane was loaded with cell lysates obtained from separate transfections. Values are the mean ± SEM of three experiments. **h** cells transfected with either control or LPA_1 siRNA were treated for 1 h with 5 µM mianserin and then exposed for 24 h to TNF-α. Cell lysates were analyzed for cleaved and uncleaved PARP. Values are the mean ± SEM of three experiments. **i** cells were treated with the test agents as indicated in a. DNA fragmentation (green color) was detected by using an in situ fluorimetric TUNEL assay. Values are expressed as percent of positive nuclei and are the mean ± SEM of four separate experiments. Bar = 50 µm. $^{***}p < 0.001$ versus control (vehicle), $^{\#}p < 0.05$, $^{\#\#}p < 0.01$, $^{\#\#\#}p < 0.001$

stimulation of ERK1/2 phosphorylation by either amitriptyline or mianserin. We then examined whether the FGFR pathway operated in the protective effect of antidepressants against the pro-apoptotic action of TNF-α. As shown in Fig. 6b, c, PD173074 (30 nM) almost completely suppressed the inhibitory effect of mianserin on TNF-α-induced PARP cleavage and markedly reduced that elicited by amitriptyline. Similarly, interruption of the ERK1/2 signal transduction pathway with the MEK1/2 inhibitor PD98059 (25 µM) curtailed the anti-apoptotic effects of both antidepressants (Fig. 6d, e).

ERK1/2 exert pro-survival actions by transcriptional and post-translational mechanisms [47]. Among the latter, phosphorylation at Thr163 of the anti-apoptotic protein Mcl-1, a Bcl-2 family member which blocks the pro-apoptotic proteins Bak and Bax [48], has been shown to enhance Mcl-1 stability against proteasomal degradation [49]. As shown in Fig. 6f, in HT22 hippocampal cells mianserin (5 µM) induced a rapid increase in the phosphorylation of Mcl-1 at Thr163. This effect was completely blocked by Ki16425 (100 nM) (Fig. 6g) and was prevented by PD 173074 (Fig. 6h) and PD98059 (Fig. 6i), indicating the mediation by LPA_1-coupled to activation of FGF-R and ERK1/2. Cell treatment with the MEK1/2 inhibitor also reduced the increase of Mcl-1 levels in the cell mitochondrial fraction elicited by a prolonged exposure to mianserin (Fig. 6j).

TNF-α activates MAP kinases to induce either cell survival or apoptosis

Time-course experiments showed that in HT22 hippocampal cells TNF-α (10 ng/ml) induced a rapid increase of ERK1/2 phosphorylation with a peak at 15 min followed by a plateau which lasted at least 3 h (Fig. 7a). This response occurred independently of LPA_1 activation, as indicated by the lack of effect by AM966 (Online Resource 6). TNF-α also caused a time-dependent increase in the phosphorylation of JNK and p38 MAPK, which peaked at 15 min and then declined (Fig. 7b, c). Cell treatment with oxoz (1 µM), an inhibitor of the MAP kinase kinase kinase (MAP3K) TAK1 [50], completely blocked TNF-α-induced JNK and ERK1/2 activation, whereas it had a slight inhibitory effect on p38 MAPK stimulation (Fig. 7 d–f).

When the role of MAP kinases in TNF-α-induced apoptosis was examined, it was found that blockade of p38 MAPK with BIRB0796 (1 µM), which inhibits all p38 MAPK isoforms [51], attenuated TNF-α-induced PARP cleavage, whereas blockade of either JNK with the selective inhibitor TCS JNK6o (10 µM) [52] or ERK1/2 with PD98059 caused an opposite effect (Fig. 7g, h). Cell transfection with a constitutively active form of ERK2 (ERK2-CA) significantly attenuated TNF-α induced PARP cleavage (Online Resource 7). These results suggest that p38 MAPK activation by TNF-α mediates a pro-apoptotic effect, whereas the stimulation of JNK and ERK1/2 conveys pro-survival signals.

JNK and ERK1/2 have been reported to phosphorylate Bcl-2 at Ser70 and this modification has been associated with an enhancement of Bcl-2 anti-apoptotic function [53]. In HT22 hippocampal cells, TNF-α increased the levels of phospho-Ser70-Bcl-2 with a kinetic profile resembling that of JNK activation (Fig. 7i). Moreover, TNF-α-induced Bcl-2 phosphorylation was blocked by TCS JNK6o, whereas PD98059 had no significant effect (Fig. 7j) indicating the involvement of JNK activation in this cytokine response.

Antidepressants potentiate TNF-α-induced activation of pro-survival signalling via JNK and ERK1/2

Pre-treatment of HT22 hippocampal cells with either mianserin or mirtazapine failed to affect basal JNK

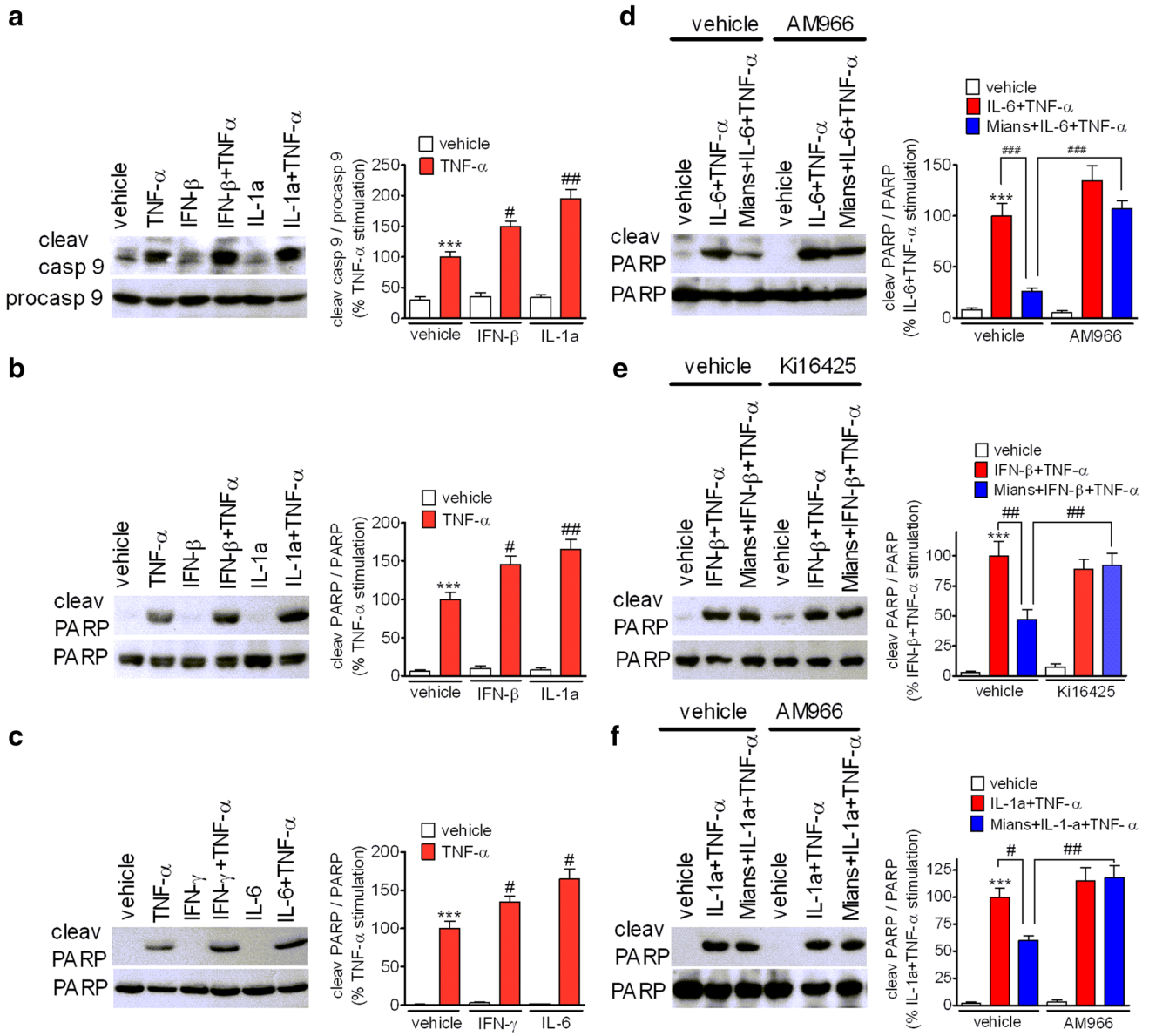

Fig. 4 Mianserin counteracts the synergistic induction of apoptosis by the combined action of pro-inflammatory cytokines. **a**–**c** HT22 cells were incubated for 24 h with TNF-α (10 ng/ml) alone or in combination with either IFN-β, IFN-γ, IL-1a or IL-6 (each used at 30 ng/ml). Cell lysates were analyzed for cleaved caspase 9, procaspase 9, cleaved and uncleaved PARP. Values are the mean ± SEM of four experiments. $^{***}p < 0.001$ versus control (vehicle), $^{\#}p < 0.05$, $^{\#\#}p < 0.01$ versus TNF-α alone. **d**–**f** cells were pre-treated with either vehicle, 100 nM AM966 or 100 nM Ki16425 for 30 min, and then exposed for 24 h to the indicated combinations of cytokines with and without 5 μM mianserin. Values are the mean ± SEM of four experiments. $^{***}p < 0.001$ versus control (vehicle), $^{\#}p < 0.05$, $^{\#\#}p < 0.01$, $^{\#\#\#}p < 0.001$

phosphorylation but markedly potentiated the activation elicited by TNF-α (Fig. 8a). A synergistic interaction in JNK activation was also observed when TNF-α was combined with either LPA or FGF-2 (Fig. 8b). Consistent with the synergistic activation of JNK, TNF-α-induced Bcl-2 phosphorylation was increased by either mianserin or mirtazapine (Fig. 8c). Cell pre-treatment with the antidepressants also enhanced ERK1/2 stimulation by TNF-α, as this response was significantly greater than the sum of the individual stimulatory effects (Fig. 8d). This synergistic interaction in ERK1/2 activation was associated with an enhanced accumulation of Mcl-1 in the mitochondrial fraction when mianserin was combined with TNF-α (Fig. 8e). Unlike JNK and ERK1/2, p38 MAPK activation by TNF-α was not affected by cell pre-treatment with either mianserin or mirtazapine (Fig. 8f).

As TAK1 appeared to mediate MAP kinases activation by TNF-α, we examined whether antidepressants and the

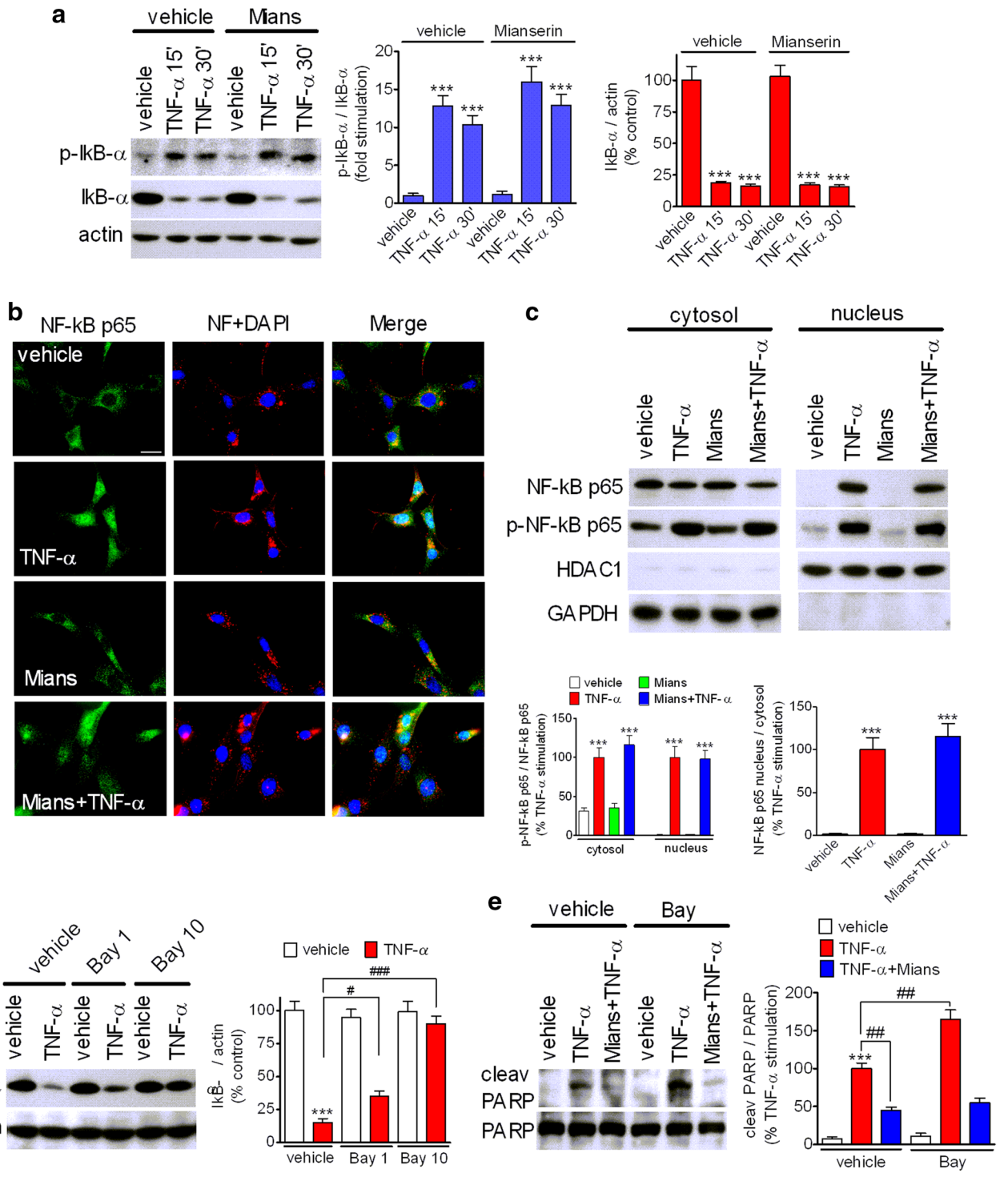

Fig. 5 Mianserin fails to inhibit TNF-α-induced activation of NF-kB pro-survival pathway. **a** HT22 hippocampal cells were pre-treated for 1 h with either vehicle or 5 μM mianserin (Mians) and then exposed to TNF-α (10 ng/ml) for the indicated periods of time. Cell extracts were analyzed for phospho(Ser32)-IkB-α (p-IkB-α), total IkB-α, and actin by Western blot. **b** cells were pre-treated for 1 h with mianserin, exposed to TNF-α for 30 min and then analyzed for NF-kB p65 subunit (green color) and NF160/200 (red color) expression by immunofluorescence. Cell nuclei were stained with DAPI. **c** cells were treated as indicated in b. Cell cytosol and nuclear fraction were prepared and the levels of phospho-(Ser536) NF-kB p65 (p-NF-kB p65), NF-kB p65, HDAC1 (a nuclear marker) and GAPDH (a cytosolic marker) were analyzed by Western blot. **d** cells were pre-treated with either vehicle or the IkB-α phosphorylation inhibitor Bay11-7085 at 1 (Bay 1) or 10 μM (Bay 10) for 1 h and then exposed to TNF-α for 30 min. **e** cells were pre-treated for 1 h with either vehicle or Bay 11-7085 (1 μM) and then exposed for 24 h to 10 ng/ml TNF-α without and with 5 μM mianserin. Values are the mean ± SEM of four experiments. $^{***}p < 0.001$ versus control (vehicle), $^{\#}p < 0.05$, $^{\#\#}p < 0.01$, $^{\#\#\#}p < 0.001$

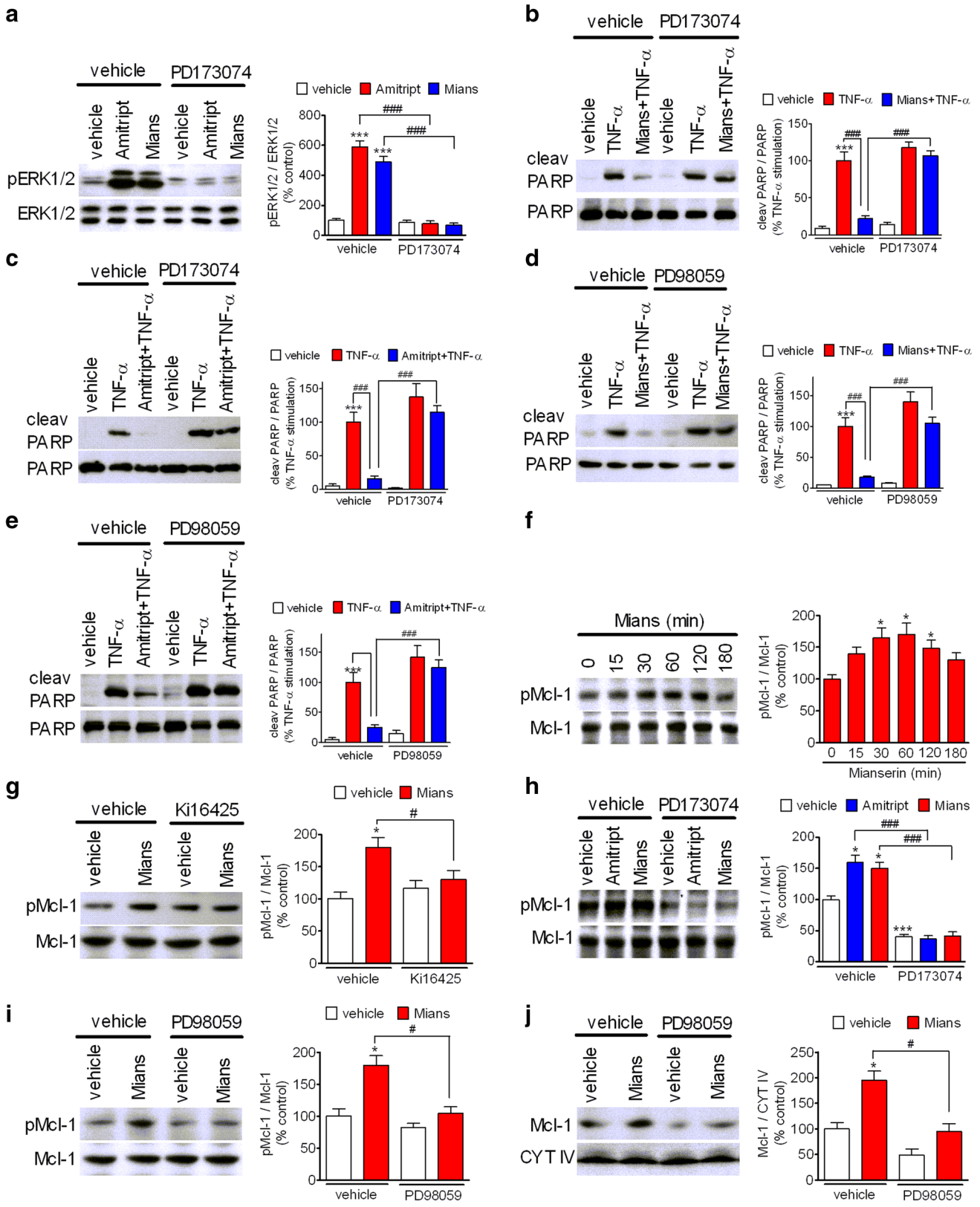

cytokine interacted at the level of this kinase. TAK1 activation occurs through multiple post-translational modifications of the core enzyme and its activator proteins TAB1 and TAB2 [54]. Cytokine-induced TAK1 activation is associated with phosphorylation of several serine and threonine residues, including Thr184 and Thr187, in the activation loop

◂**Fig. 6** The anti-apoptotic effect of antidepressants involves FGF-R and ERK1/2 activities. **a** HT22 hippocampal cells were pre-incubated for 1 h with either vehicle or the FGF-R tyrosine kinase inhibitor PD173074 (30 nM) and then exposed to either amitriptyline (Amitript) (15 μM) or mianserin (5 μM) (Mians) for 5 min. Densitometric ratios of phospho-ERK1/2 (pERK1/2) levels normalized to total ERK1/2 levels are expressed as percent of control (vehicle). **b**–**e** cells were preincubated for 1 h with either vehicle, PD173074 (30 nM) (b and c) or the MEK1/2 inhibitor PD98059 (25 μM) (**d, e**) and then treated for 1 h with either vehicle, 5 μM mianserin, or 10 μM amitriptyline. Thereafter, cells were exposed for 24 h to either vehicle or 10 ng/ml TNF-α. **f** cells were incubated for the indicated periods of time with 5 μM mianserin. Zero time samples were treated with vehicle and used as control. Cell lysates were analyzed for phospho-(Thr163)-Mcl-1 (pMcl-1) and Mcl-1 protein expression. **g**–**i** cells were pre-incubated with either vehicle, 100 nM Ki16425 (for 30 min) (g), 30 nM PD173074 (h) or 25 μM PD98059 (i) (both for 1 h) and then exposed to either vehicle or 5 μM mianserin for 30 min. **j** cells were pre-incubated with PD98059 as indicated in i and then exposed to either vehicle or 5 μM mianserin for 12 h. Cell were lysed and the levels of Mcl-1 and cytochrome oxidase IV (CYT IV) were measured in a mitochondrial fraction. Values are the mean ± SEM of four experiments. $^{*}p<0.05$, $^{***}p<0.001$ versus control (vehicle), $^{\#}p<0.05$, $^{\#\#\#}p<0.001$

of the kinase, and Thr187 phosphorylation correlates with TAK1 stimulation by TNF-α [55]. As shown in Fig. 8g, in HT22 hippocampal cells TNF-α (10 ng/ml) increased the levels of phospho-Thr184/187-TAK1 and this response was potentiated by cell pre-treatment with either mianserin or mirtazapine, which per se displayed only a modest stimulatory effect.

Discussion

The binding of TNF-α to TNF receptors is known to activate a wide array of signalling pathways that can promote either cell death or pro-survival effects, and the cellular response to the cytokine may be the result of the functional interaction between the opposing pathways [1–3]. In the present study, we show that through activation of the LPA_1 receptor the antidepressants mianserin, mirtazapine and amitriptyline curtail TNF-α-induced neuronal apoptosis and this protective effect occurs, at least in part, by potentiating the pro-survival branch of TNF-α signalling.

Both TNFR1 and TNFR2 have been found to be present in HT22 hippocampal cells and hippocampal neurons [15, 56]. Radioligand binding studies have shown that soluble TNF-α preferentially binds to TNFR1 [57], and functional studies have reported that soluble TNF-α, used at concentrations (1–10 ng/ml) similar to that employed in the present study, predominantly signals through TNFR1 in cells expressing both TNF receptors [58]. On the other hand, it has been demonstrated that the transmembrane form of TNF-α is the prime activating ligand of TNFR2 [4]. Thus, it is likely that the apoptotic response to TNF-α observed in the present study was mediated by TNFR1. This conclusion is further supported by the finding that human TNF-α, which selectively activates murine TNFR1 over TNFR2 [40], mimicked the cytotoxic effect of mouse TNF-α. The present results are in line with the previous observation that in HT22 hippocampal cells TNFR1 is the receptor isoform that mediates the mitochondrial dysfunction in response to TNF-α [15], and provide further support to the view that selective activation of TNFR1 signalling is associated with neuronal cell death [11, 16, 59, 60].

A key finding of the present study is that antidepressants inhibit TNF-α-induced apoptosis by acting through LPA_1. This observation is consistent with our recent discovery that LPA_1 is a critical mediator of intracellular signalling and pro-survival response elicited by different classes of antidepressants [31–33]. The involvement of LPA_1 in the actions of these drugs was assessed by using selective receptor antagonists and gene silencing with siRNA. A number of independent studies have provided evidence that signalling through LPA_1 has neuroprotective effects. Thus, it has been shown that mice deficient of LPA_1 display increased cortical apoptosis [61]. Stimulation of LPA_1 rescues H19-7 hippocampal cells from apoptosis occurring under non-permissive temperature [62]. Moreover, in hippocampal neurons activation of endogenously expressed LPA_1 mediates the protective effects of tetracyclic antidepressants against apoptosis induced by nutrient deprivation stress [33]. The finding that LPA_1 and TNFR1 signalling can cross-talk in the regulation of the apoptotic response is supported by the observation that both receptors are co-expressed in a large fraction of HT22 hippocampal cells. Although not specifically investigated, a co-localization may also occur in hippocampal neurons, as these cells were found to express both LPA_1 and TNFR1 [33, 56].

Neuroinflammation is sustained by the combined action of multiple cytokines which may cooperate in promoting brain damage and neuronal death. We found that in HT22 hippocampal cells the pro-apoptotic response to TNF-α was potentiated when the cytokine was combined with either IFN-β, IFN-γ, IL-1a or IL-6. Like TNF-α, these pro-inflammatory cytokines have been found to be elevated in patients with major depression and have been implicated in the pathogenesis of this disorder [24]. It is noteworthy that antidepressant-induced LPA_1 activation reduced the enhanced PARP cleavage resulting from each cytokine combination. These results suggest that the pro-survival signals activated by the antidepressant-LPA_1 axis is capable of restrict TNF-α-induced neuronal apoptosis when this response is up-regulated by the coincident actions of other pro-inflammatory cytokines.

Different lines of evidence indicate that antidepressant-triggered LPA_1 pro-survival signalling inhibits TNF-α-induced neuronal death by opposing the activation of the

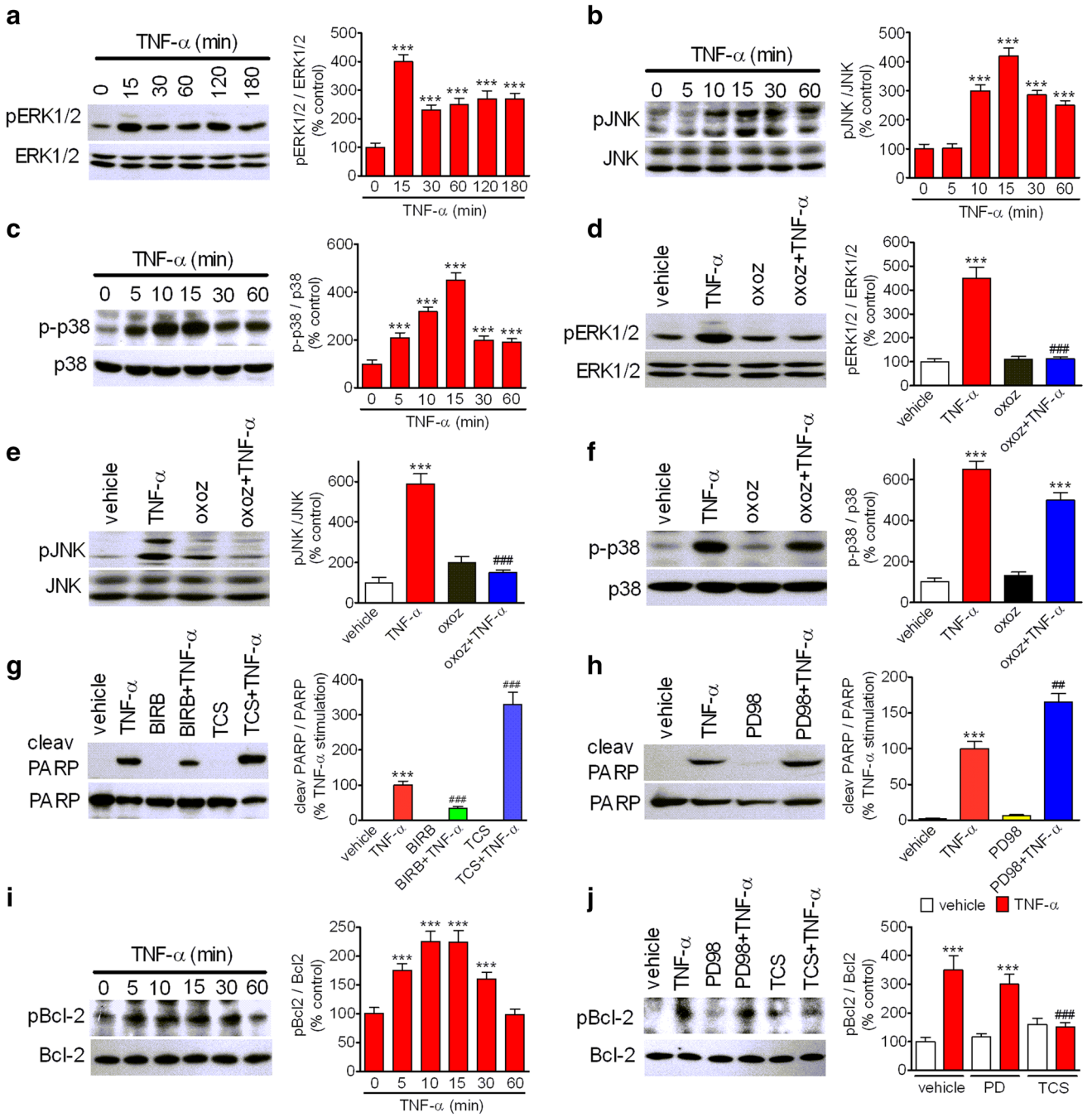

Fig. 7 TNF-α activates MAP kinases through TAK1 to promote either cell survival or apoptosis. **a–c** HT22 cells were incubated for the indicated periods of time with 10 ng/ml TNF-α and cell extracts were analyzed for dually phosphorylated ERK1/2 (pERK1/2), total ERK1/2, phospho-JNK (pJNK), total JNK, phospho-p38 MAPK (p-p38) and total p38 MAPK (p38). Values are the mean ± SEM of three experiments. **d–f** cells were pre-incubated for 30 min with either vehicle or 5Z-7-oxozeaenol (oxoz) (100 nM) and then treated for 15 min with either vehicle or 10 ng/ml TNF-α. Values are the mean ± SEM of four experiments. **g** and **h** cells were pre-incubated for 1 h with either vehicle, BIRB0796 (BIRB) (1 μM), TCS JNK6o (TCS) (10 μM), or PD98059 (PD98) (25 μM), and then exposed for 24 h to either vehicle or 10 ng/ml TNF-α. Values are the mean ± SEM of five experiments. **i** cells were incubated in the presence of 10 ng/ml TNF-α for the indicated periods of time. Zero time samples were treated with vehicle and used as control. Cell lysates were analyzed for phospho-(Ser70)-Bcl-2 (pBcl-2) and total Bcl-2 levels. Values are the mean ± SEM of three experiments. **j** cells were pre-incubated for 1 h with either vehicle, PD98059 (25 μM) or TCS JNK6o (10 μM) and then exposed for 15 min to either vehicle or 10 ng/ml TNF-α. Values are the mean ± SEM of four experiments. $^{***}p < 0.001$ versus control (vehicle); $^{\#\#}p < 0.01$, $^{\#\#\#}p < 0.001$ versus TNF-α alone

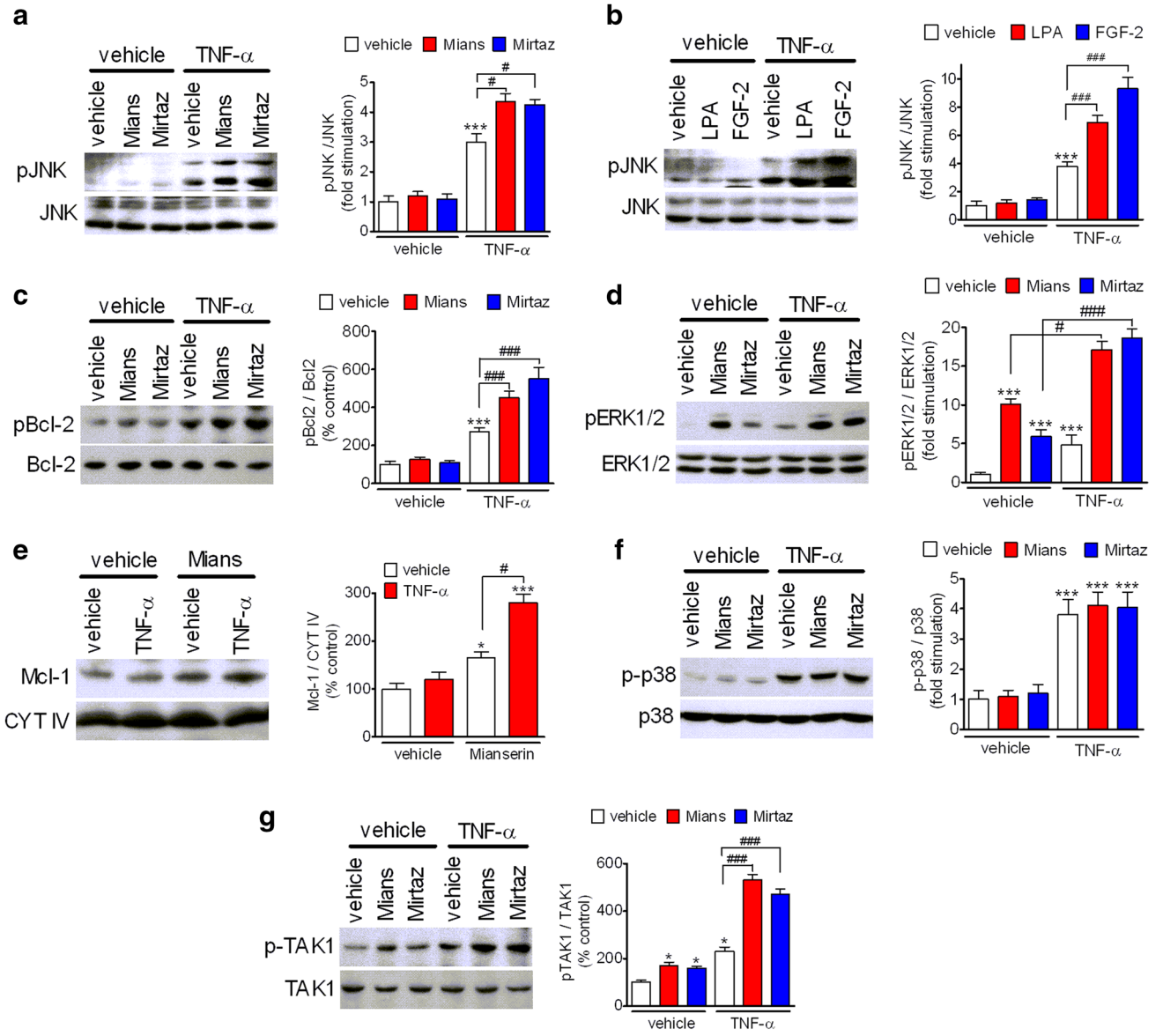

Fig. 8 Antidepressants potentiate TNF-α-induced activation of JNK and ERK1/2 pro-survival signalling. **a** HT22 cells were pre-incubated for 1 h with either vehicle, 5 μM mianserin or 20 μM mirtazapine and then exposed for 15 min to 10 ng/ml TNF-α. Cell lysates were analyzed for phospho-JNK and total JNK. Values are the mean ± SEM of four experiments. **b** cells were pre-incubated with either vehicle, 1 μM LPA or 10 ng/ml FGF-2 for 1 h and then exposed to 10 ng/ml TNF-α for 15 min. Values are the mean ± SEM of three experiments. **c** cells were pre-incubated as indicated in a, and then exposed to TNF-α for 15 min. Cell lysates were analyzed for phospho-(Ser70)-Bcl-2 (pBcl-2) and total Bcl-2 levels. Values are the mean ± SEM of four experiments. **d** cells were treated as indicated in a. Cell lysates were analyzed for phospho-ERK1/2 and total ERK1/2 levels. Values are the mean ± SEM of four experiments. **e** cells were pre-incubated with either vehicle or 5 μM mianserin for 1 h and then exposed to either vehicle or 10 ng/ml TNF-α for 12 h. A mitochondrial fraction was prepared and analyzed for the levels of Mcl-1 and cytochrome oxidase IV (CYT IV). Values are the mean ± SEM of four experiments. **f** cells were treated as indicated in a, and cell lysates were analyzed for phospho-p38 MAPK and total p38 MAPK. Values are the mean ± SEM of four experiments. **g** cells were treated as indicated in a, and cell lysates were analyzed for phospho-(Thr184/187)-TAK1 (pTAK1) and total TAK1. Values are the mean ± SEM of four experiments. $^{*}p < 0.05$, $^{***}p < 0.001$ versus control (vehicle), $^{\#}p < 0.05$, $^{\#\#\#}p < 0.001$

mitochondrial-dependent intrinsic apoptotic pathway. Thus, along the apoptotic cascade initiated by TNF-α, mianserin had no effect on the activation of caspase 8, suggesting that the antidepressant did not interfere with the processes occurring upstream this event, including TNF-α-induced TNFR1 activation and internalization, FADD association and pro-caspase 8 recruitment. On the other hand, mianserin markedly inhibited the loss of mitochondrial membrane

potential, the release of cytochrome c from mitochondria and the activation of pro-caspase 9 elicited by the cytokine. By acting through LPA_1-coupled to ERK1/2 mianserin increased the steady state mitochondrial levels of Mcl-1, an anti-apoptotic protein that acts by sequestering Bak and Bax, two inducers of mitochondrial outer membrane permeability [48]. Previous studies in non-neuronal cells have shown that up-regulation of Mcl-1 was sufficient to effectively counteract the induction of apoptosis by either TNF-α or TRAIL [63, 64]. Thus, the data suggest that in HT22 hippocampal cells LPA_1 signalling activated by antidepressants may attenuate the TNF-α initiation of the intrinsic apoptotic pathway by enhancing the activity of proteins that preserve the mitochondrial outer membrane permeability.

Treatment of HT22 hippocampal cells with mianserin failed to inhibit the activation of the NF-kB pathway, as indicated by the lack of significant effects on the stimulation of IkB-α phosphorylation and degradation, and the inability of the antidepressant to prevent the nuclear translocation and phosphorylation of the NF-kB p65 subunit. In agreement with previous studies showing that in TNF-α-treated cells NF-kB mediates neuroprotective effects [65], blockade of NF-kB activation with Bay 11-7085 enhanced the pro-apoptotic response of TNF-α. The treatment, however, did not change the pro-survival action of mianserin. These results indicate that antidepressant-stimulated LPA_1 signalling selectively curtails the pro-apoptotic cascade triggered by TNF-α, while leaving intact the cytokine ability to counter-regulate its own neurotoxicity through activation of NF-kB.

Stimulation of ERK1/2 mediated by LPA_1-induced FGF-R transactivation appeared to play a major role in the intracellular mechanisms mediating the protective effect of antidepressants against TNF-α-induced apoptosis. In fact, pharmacological blockade of either FGF-R tyrosine kinase activity or MEK1/2 activity prevented the anti-apoptotic effects of mianserin and amitriptyline. By acting through LPA_1 and ERK1/2, mianserin stimulated the phosphorylation of Mcl-1 at Thr163, which has been shown to increase the stability of the protein. This effect may account for the increased amount of Mcl-1 found in the mitochondrial fraction following treatment of HT22 hippocampal cells with mianserin.

Activation of MAP kinases is known to be an important route by which TNF-α can induce either cell death or survival [66, 67]. In HT22 hippocampal cells, TNF-α caused a rapid activation of ERK1/2, JNK and p38 MAPK, as indicated by their enhanced phosphorylation state. Blockade of ERK1/2 activation potentiated TNF-α-induced PARP cleavage whereas expression of ERK2-CA attenuated this response, supporting the pro-survival function of these kinases. A similar finding was reported in previous studies showing that in HeLa cells the stimulation of ERK1/2 activity by Fas, TNF and TRAIL receptors antagonizes the apoptotic signalling by suppressing the activation of the caspase effector machinery [68]. A protective role appeared to be played also by JNK, as blockade of its activity yielded a greater PARP cleavage in response to TNF-α. JNK activation by TNF-α displayed an early peak and was transient, a kinetic profile that has been linked to a pro-survival function [69]. Moreover, in HT22 hippocampal cells TNF-α-induced JNK stimulation was associated with an increased phosphorylation of the anti-apoptotic protein Bcl-2 at Ser70, a site located within the flexible loop domain of the protein. The phosphorylation of Bcl-2 at this site by either JNK or ERK1/2 has been reported to enhance the Bcl-2 binding to Bim and Bax, thus potentiating its anti-apoptotic activity [70]. Unlike ERK1/2 and JNK, TNF-α-activated p38 MAPK appeared to transduce a pro-apoptotic response. A cytotoxic outcome mediated by p38 MAPK activation has been observed in non-neuronal and neural stem cells exposed to TNF-α [71, 72]. Collectively, these results indicate that MAP kinases play divergent roles in the regulation of HT22 hippocampal cell survival by TNF-α.

A unique feature of the anti-apoptotic signalling triggered by antidepressants through LPA_1 is the ability to interact synergistically with TNF-α in the activation of the pro-survival JNK and ERK1/2 pathways. The positive interaction appeared to translate into a stronger inhibitory constraint on the intrinsic apoptotic pathway, as it was accompanied by an enhanced mitochondrial Mcl-1 accumulation and an increased phosphorylation / activation of Bcl-2. We have found that TNFR1 and LPA_1 signalling also cooperate in promoting TAK1 phosphorylation at the Thr184/187 activating site. Although the precise mechanisms mediating this effect remain to be elucidated, the synergistic stimulation of TAK1 may be responsible for the potentiation of JNK and ERK1/2 activation. Interestingly, p38 MAPK activation by TNF-α was found to be only marginally reduced by TAK1 inhibition, indicating the involvement of mechanisms distinct from TAK1 activation. Nonetheless, this finding is consistent with the observation that TNF-α-induced p38 MAP kinase activation was not enhanced by pre-treatment with the antidepressants.

In conclusion, the present study demonstrates for the first time that in neuronal cells TNF-α-induced activation of the intrinsic apoptotic cascade is curtailed by antidepressants acting through a mechanism involving LPA_1-mediated FGF-R trans-activation, ERK1/2 signalling and a synergistic interaction with cytokine-activated pro-survival pathways. This mechanism is triggered by antidepressant concentrations that are reached in the brain following clinically relevant doses and therefore it may contribute to the therapeutic efficacy of the drugs. Moreover, the present study suggests that the potentiation of LPA_1 signalling may constitute a new approach for the control of neuronal damage elicited by TNF-α/TNFR1 activity.

Funding This study was funded by Regione Autonoma della Sardegna, Italy. L.R. no. 7/2007 (CRP10810/2012) and by Universita' degli Studi di Cagliari, Italy, FIR 2017.

Compliance with Ethical Standards

Conflict of interest The authors declare that they have no conflict of interest.

References

1. Aggarwal BB, Gupta SC, Kim JH (2012) Historical perspectives on tumor necrosis factor and its superfamily: 25 years later, a golden journey. Blood 119:651–665
2. Bradley JR (2008) TNF-mediated inflammatory disease. J Pathol 214:149–160
3. Faustmann DL, Davis M (2013) TNF receptor 2 and disease: autoimmunity and regenerative medicine. Front Immunol 4:478. https://doi.org/10.3389/fimmu.2013.00478
4. Grell M, Douni E, Wajant H, Lohden M, Clauss M, Maxeiner B, Georgopulos S, Lesslauer W, Kollias G, Pfizenmaier K, Scheurich P (1995) The transmembrane form of tumor necrosis factor is the prime activating ligand of the 80 kDa tumor necrosis factor receptor. Cell 83:793–802
5. McCoy MK, Tansey MG (2008) TNF signalling inhibition in the CNS: implications for normal brain function and neurodegenerative disease. J Neuroinflamm 5:45. https://doi.org/10.1186/1742-2094-5-45
6. Park KM, Bowers WJ (2010) Tumor necrosis factor-alpha mediated signaling in neuronal homeostasis and dysfunction. Cell Sign 22:977–983
7. Probert L (2015) TNF and its receptors in the CNS: the essential, the desiderable and the deleterious effects. Neuroscience 302:2–22
8. Cheng B, Christakos S, Mattson MP (1994) Tumor necrosis factors protect neurons against metabolic-excitotoxic insults and promote maintenance of calcium homeostasis. Neuron 12:139–153
9. Barger SW, Horster D, Furukawa K, Goodman Y, Krieglstein J, Mattson MP (1995) Tumor necrosis factors α and β protect neurons against amyloid β-peptide toxicity: evidence for involvement of a kB-binding factor and attenuation of peroxide and Ca^{2+} accumulation. Proc Natl Acad Sci USA 92:9328–9332
10. Tamatani M, Che YH, Matsuzaki H, Ogawa S, Okado H, Miyake S-i, Mizuno T, Tohyama M (1999) Tumor necrosis factor induces Bcl-2 and Bcl-x expression through NF-κB activation in primary hippocampal neurons. J Biol Chem 274:8531–8538
11. Marchetti L, Klein M, Schlett K, Pfizenmaier K, Eisel ULM (2004) Tumor necrosis factor (TNF)-mediated neuroprotection against glutamate-induced excitotoxicity is enhanced by N-methyl-D-aspartate receptor activation. J Biol Chem 279:32869–32881
12. Zhao X, Bausano B, Pike BR, Newcomb-Fernandez JK, Wang KKW, Shohami E, Ringger NC, DeFord SM, Anderson DK, Hayes RL (2001) TNF-α stimulates caspase-3 activation and apoptotic cell death in primary septo-hippocampal cultures. J Neurosci Res 64:121–131
13. Reimann-Philipp U, Ovase R, Weigel PH, Grammas P (2001) Mechanisms of cell death in primary cortical neurons and PC12 cells. J Neurosci Res 64:654–660
14. Olmos G, Llado' J (2014) Tumor necrosis factor alpha: a link between neuroinflammation and excitotoxicity. Mediat Inflamm ID 861231 https://doi.org/10.1155/2014/861231
15. Doll DN, Rellick SL, Barr TL, Ren X, Simpkins JW (2015) Rapid mitochondrial dysfunction mediates TNF-alpha-induced neurotoxicity. J Neurochem 132:443–451
16. Badiola N, Malagelada C, Llecha N, Hidalgo J, Comella JX, Sabria J, Rodriguez-Alvarez J (2009) Activation of caspase-8 by tumour necrosis factor receptor 1 is necessary for caspase-3 activation and apoptosis in oxygen-glucose deprived cultured cortical cells. Neurobiol Dis 35:438–447
17. Liu S, Wang X, Li Y, Su L, Yu X, Ge L, Li J, Zhu Y, He S (2014) Necroptosis mediates TNF-induced toxicity of hippocampal neurons. BioMed Res Int. https://doi.org/10.1155/2014/290182
18. Fischer R, Kontermann RE, Maier O (2015) Targeting sTNF/TNFR1 signaling as a new therapeutic strategy. Antibodies 4:48–70
19. Raison CL, Miller AH (2011) Is depression an inflammatory disorder ? Curr Psychiatry Rep 13:467–475
20. Dowlati Y, Herrmann N, Swardfager W, Liu H, Sham L, Reim EK, Lanctot KL (2010) A meta-analysis of cytokines in major depression. Biol Psychiatry 67:446–457
21. Liu Y, Chun-Man Ho R, Mak A (2012) Interleukin (IL)-6, tumor necrosis factor alpha (TNF-α) and soluble interleukin-2 receptor (sIL-2R) are elevated in patients with major depressive disorder: a meta-analysis and meta-regression. J Affect Disord 139:230–239
22. Simen BB, Duman CH, Simen AA, Duman RS (2006) TNFα signaling in depression and anxiety: behavioral consequences of individual receptor targeting. Biol Psychiatry 59:775–785
23. Silverman MN, Macdougall MG, Hu F, Pace TW, Raison CL, Miller AH (2007) Endogenous glucocorticoids protect against TNF-alpha-induced increases in anxiety-like behavior in virally infected mice. Mol Psychiatry 12:408–417
24. Miller AH, Maleric V, Raison CL (2009) Inflammation and its discontent: the role of cytokines in the pathophysiology of major depression. Biol Psychiatry 65:732–741
25. Cacci E, Claasen JH, Kokaia Z (2005) Microglia-derived tumor necrosis factor-alpha exaggerates death of newborn hippocampal progenitors cells in vitro. J Neurosci Res 80:273–277
26. Liu YP, Lin HI, Tzeng SF (2005) Tumor necrosis factor-alpha and interleukin – 18 modulate neuronal cell fate in embryonic neural progenitor culture. Brain Res 1054:152–158
27. Iosif RE, Ekdahl CT, Ahlenius H, Pronk CJ, Bonde S, Kokaia Z, Jacobsen SE, Lindvall O (2006) Tumor necrosis factor receptor 1 is a negative regulator of progenitor proliferation in adult hippocampal neurogenesis. J Neurosci 26:9703–9712
28. Xia Z, DePierre JW, Nassberger L (1996) Tricyclic antidepressants inhibit IL-6, IL-1 beta and TNF-alpha release in human blood monocytes and IL-2 and interferon-gamma in T cells. Immunopharmacology 34:27–37
29. Kenis G, Maes M (2002) Effects of antidepressants on the production of cytokines. Int J Neuropsychopharmacol 5:401–412
30. Hwang J, Zheng LT, Ock J, Lee MG, Kim S-H, Lee H-W, Lee W-H, Park H-C, Suk K (2008) Inhibition of glial inflammatory activation and neurotoxicity by tricyclic antidepressants. Neuropharmacology 55:826–834
31. Olianas MC, Dedoni S, Onali P (2015) Antidepressants activate the lysophosphatidic acid receptor LPA_1 to induce insulin-like growth factor-I receptor transactivation, stimulation of ERK1/2 signaling and cell proliferation in CHO-K1 fibroblasts. Biochem Pharmacol 95:311–323
32. Olianas MC, Dedoni S, Onali P (2016) LPA_1 mediates antidepressant-induced ERK1/2 signaling and protection from oxidative stress in glial cells. J Pharmacol Exp Ther 359:340–353
33. Olianas MC, Dedoni S, Onali P (2017) LPA_1 is a key mediator of intracellular signalling and neuroprotection triggered by

tetracyclic antidepressants in hippocampal neurons. J Neurochem 143:183–197
34. Yung YC, Stoddard NC, Mirendil H, Chun J (2015) Lysophosphatidic acid signaling in the nervous system. Neuron 85:669–682
35. Moreno-Fernandez RD, Tabbai S, Castilla-Ortega E, Perez-Martin M, Estivill-Torrus G, Rodriguez de Fonseca F, Santin LJ, Pedraza C (2018) Stress, depression, resilience and aging: a role for the LPA-LPA$_1$ pathway. Curr Neuropharmacol 16, https://doi.org/10.2174/1570159X15666170710200352
36. Robinson MJ, Stippec SA, Goldsmith E, White MA, Cobb MH (1998) A constitutively active and nuclear form of the MAP kinase ERK2 is sufficient for neurite outgrowth and cell transformation. Curr Biol 8:1141–1150
37. Olianas MC, Dedoni S, Onali P (2016) Protection from interferon-β-induced neuronal apoptosis through stimulation of muscarinic acetylcholine receptors coupled to ERK1/2 activation. Br J Pharmacol 173:2910–2928
38. Dedoni S, Olianas MC, Onali P (2014) Interferon-β counter-regulates its own pro-apoptotic action by activating p38MAPK signalling in human SH-SY5Y neuroblastoma cells. Apoptosis 19:1509–1526
39. Dedoni S, Olianas MC, Ingianni A, Onali P (2014) Type I interferons up-regulate the expression and signalling of p75NTR/TrkA receptor complex in differentiated human SH-SY5Y neuroblastoma cells. Neuropharmacology 79:321–334
40. Lewis M, Tartaglia LA, Lee A, Bennett GL, Rice GC, Wong GH, Chen EY, Goeddel DV (1991) Cloning and expression of cDNAs for two distinct murine tumor necrosis factor receptors demonstrate one receptor is species specific. Proc Natl Acad Sci USA 88:2830–2834
41. Qian Y, Hamilton M, Sidduri A et al (2012) Discovery of highly selective and orally active lysophosphatidic acid receptor-1 antagonists with potent activity on human lung fibroblasts. J Med Chem 55:7920–7939
42. Kantari C, Walczak H (2011) Caspase-8 and Bid: caught in the act between death receptors and mitochondria. Biochim Biophys Acta 1813:558–563
43. Adams JM (2003) Ways of dying: multiple pathways to apoptosis. Genes Dev 17:2481–2495
44. Wajant H, Pfizenmaier K, Scheurich P (2003) Tumor necrosis factor signaling. Cell Death Diff 10:45–65
45. Christian F, Smith EL, Carmody RJ (2016) The regulation of NF-kB subunits by phosphorylation. Cells 5:12. https://doi.org/10.3390/cells5010012
46. Pierce JW, Schoenleber R, Jesmok G, Best J, Moore SA, Collins T, Gerritsen ME (1997) Novel inhibitors of cytokine-induced IkBα phosphorylation and endothelial cell adhesion molecule expression show anti-inflammatory effects *in vivo*. J Biol Chem 272:21096–21103
47. Lu Z, Xu S (2006) ERK1/2 MAP kinases in cell survival and apoptosis. IUBMB Life 58:621–631
48. Thomas LW, Lam C, Edwards SW (2010) Mcl-1: the molecular regulation of protein function. FEBS Lett 584:2981–2989
49. Domina AM, Vrana JA, Gregory MA, Hann SR, Craig RW (2004) MCL1 is phosphorylated in the PEST region and stabilized upon ERK activation in viable cells, and at additional sites with cytotoxic okadaic acid or taxol. Oncogene 23:5301–5315
50. Ninomiya-Tsuji J, Kajino T, Ono K, Ohtomo T, Matsumoto M, Shiina M, Mihara M, Tsuchiya M, Matsumoto K (2003) A resorcylic acid lactone, 5Z-7-oxozeaenol, prevents inflammation by inhibiting the catalytic activity of TAK1 MAPK kinase kinase. J Biol Chem 278:18485–18490
51. Bain J, Plater L, Elliott M, Shpiro N, Hastie CJ, McLauchlan H, Klevernic I, Arthur JSC, Alessi DR, Cohen P (2007) The selectivity of protein kinase inhibitors: a further update. Biochem J 408:297–315
52. Szczepankiewicz BG, Kosogof C, Nelson LTJ et al (2006) Aminopyridine-based c-Jun N-terminal kinase inhibitors with cellular activity and minimal cross-kinase activity. J Med Chem 49:3563–3580
53. Deng X, Xiao L, Lang W, Gao F, Ruvolo P, May WS Jr (2001) Novel role for JNK as a stress-activated Bcl2 kinase. J Biol Chem 276:23681–23688
54. Sakurai H (2012) Targeting of TAK1 in inflammatory disorders and cancer. Cell 33:522–530
55. Singhirunnusorn P, Suzuki S, Kawasaki N, Saiki I, Sakurai H (2005) Critical roles of threonine 187 phosphorylation in cellular stress-induced rapid and transient activation of transforming growth factor-β-activated kinase 1 (TAK1) in a signaling complex containing TAK1-binding protein TAB1 and TAB2. J Biol Chem 280:7359–7368
56. Neumann H, Schweigreiter R, Yamashita T, Rosenkranz K, Wekerle H, Barde Y-A (2002) Tumor necrosis factor inhibits neurite outgrowth and branching of hippocampal neurons by a Rho-dependent mechanism. J Neurosci 22:854–862
57. Grell M, Wajant H, Zimmermann G, Scheurich P (1998) The type 1 receptor (CD120a) is the high-affinity receptor for soluble tumor necrosis factor. Proc Natl Acad Sci USA 95:570–575
58. Thoma B, Grell M, Pfizenmaier K, Scheurich P (1990) Identification of a 60-kD tumor necrosis factor (TNF) receptor as the major signal transducing component in TNF responses. J Exp Med 172:1019–1023
59. Yang L, Lindholm K, Konishi Y, li R, Shen Y (2202) Target depletion of distinct tumor necrosis factor receptor subtypes reveals hippocampal neuron death and survival through different signal transduction pathways. J Neurosci 22:3025–3032
60. Dong Y, Fischer R, Naude PJW, Maier O, Nyakas C, Duffey M, Van der Zee EA, Dekens D, Douwenga W, Herrmann A, Guenzi E, Kontermann RE, Pfizenmaier K, Eisel ULM (2016) Essential protective role of tumor necrosis factor receptor 2 in neurodegeneration. Proc Natl Acad Sci 113:12304–12309
61. Estivill-Torrus G, Llebrez-Zayas P, Matas-Rico E, Santin L, Pedraza C, De Diego I, Del Arco I, Fernandez-Llebrez P, Chun J, Rodriguez De Fonseca F (2008) Absence of LPA$_1$ signaling results in defective cortical development. Cereb Cortex 18:938–950
62. Sun Y, Nam J-S, Han D-H, Kim N-H, Choi H-K, Lee JK, Rhee HJ, Huh S-O (2010) Lysophosphatidic acid induces upregulation of Mcl-1 and protects apoptosis in a PTX-dependent manner in H19-7 cells. Cell Signal 22:484–494
63. Kodama Y, Taura K, Miura K, Schnabel B, Osawa Y, Brenner DA (2009) Antiapoptotic effect of c-Jun N-terminal kinase-1 through Mcl-1 stabilization in TNF-induced hepatocyte apoptosis. Gastroenterology 136:1423–1434
64. Taniai M, Grambihler A, Higuchi H, Werneburg N, Bronk SF, Farrugia DJ, Kaufmann SH, Gores GJ (2004) Mcl-1 mediates tumor necrosis factor-related apoptosis-inducing ligand resistance in human cholangiocarcinoma cells. Cancer Res 64:3517–3524
65. Mattson MP, Meffert MK (2006) Roles for NF-kB in nerve cell survival, plasticity, and disease. Cell Death Differ 13:852–860
66. Sabio G, Davis RJ (2014) TNF and MAP kinase signaling pathways. Semin Immunol 26:237–245
67. Varfolomeev EE, Ashkenazi A (2004) Tumor necrosis factor: an apoptosis JuNKie. ? Cell 116:491–497
68. Tran SEF, Holmstrom TH, Ahonen M, Kahari V-M, Eriksson JE (2001) MAPK/ERK overrides the apoptotic signaling from Fas, TNF, and TRAIL receptors. J Biol Chem 276:16484–16490
69. Ventura JJ, Hubner A, Zhang C, Flavell RA, Shokat KM, Davis RJ (2006) Chemical genetic analysis of the time course of signal transduction by JNK. Mol Cell 21:701–710

70. Dai H, Ding H, Meng XW, Lee S-H, Schneider PA, Kaufmann SH (2013) Contribution of Bcl-2 phosphorylation to Bak binding and drug resistance. Cancer Res 73:6998–7008
71. Chen N-n, Wei F, Wang L, Cui S, Wan Y, Liu S (2016) Tumor necrosis factor alpha induces neural stem cell apoptosis through activating p38 MAPK pathway. Neurochem Res 41:3052–3062
72. Grethe S, Ares MPS, Anderson T, Porn-Ares I (2004) p38 MAPK mediates TNF-induced apoptosis in endothelial cells via phosphorylation and downregulation of Bcl-x_L. Exp Cell Res 298:632–642